Journal Name

ARTICLE

Organic semiconductors for biological sensing

Jorge Borges-González,† Christina J. Kousseff† and Christian B. Nielsen*

Received 00th January 20xx,
Accepted 00th January 20xx

DOI: 10.1039/x0xx00000x

www.rsc.org/

In this review, we provide an overview of conjugated organic semiconductors and their applications in biological sensing with a primary focus on the role of the organic semiconductor. We cover work carried out with polymers as well as small molecules, from the well-established and commercially available systems to the emerging and recently developed materials.

1. Introduction

Nowadays, a wide range of relevant biological molecules can be conveniently detected or quantified in robust, miniaturised, portable devices that generate a digital read-out. The main applications are found in medical diagnostics, especially for point-of-care testing[1] as the glucose sensors for diabetic patients, but also in food safety, environmental control, drug discovery or agriculture analysis.

1.1 Advantageous features of organic semiconductors

A huge amount of progress on biological sensors has been based on the miniaturization of silicon microelectronics. On the other hand, novel features are demanded in terms of flexibility, ease of processing, biocompatibility and mixed ion and electron conductivity,[2–4] which can render organic materials superior to inorganic alternatives. After some thirty years of development, some of these organic semiconductors have reached carrier mobilities in the range of polycrystalline silicon (> 10 $cm^2 V^{-1} s^{-1}$), combined with high stability.[5–8] But unlike their inorganic counterparts, organic materials can be deposited on plastic or glass substrates at low temperatures from vapour (small molecules) or solutions (polymers), which reduces the cost of fabrication and enables the making of disposable sensors. Flexible polymers have been shown to preserve high conductivity under the repeated strain that is natural in biological tissues, which has led to a wide range of stretchable, wearable devices mimicking human skin.[9] At the same time, this minimises the adverse reaction that may be caused by an implanted device and contributes mechanical robustness.[10,11]‡ Besides the mechanical advantages, the properties of organic materials can be extensively modulated in the stages of their chemical synthesis (both in the conjugated backbone and the side groups),[12] film deposition or by doping. For example, their solubility is commonly improved with the introduction of long or branched alkyl side chains; and the hydrophilicity of the film, and hence its capacitance, can be increased with glycol side chains.[13,14]

Finally, organic semiconductors provide ideal contact between the biological media, where ion fluxes elicit functional electrical signals, and the devices, which depend on electron conduction. The π-conjugated backbone enables electron conduction, whereas ion uptake in the bulk of the porous film (which can be further enhanced by water swelling) supports ion conduction and increases the effective surface area. Ultimately, this leads to low impedance contacts[15] and better signal-to-noise ratios. This property was initially implemented in biological applications by coating an electrode with a conducting polymer for potentiometric sensing,[16] but it will be shown below that this can be extended to the application of organic electronic devices.

1.2 Devices: an overview

Along with the potentiometric sensors mentioned above, the other first applications of organic semiconductors were based on conductometric sensors, in the form of a simple device, the chemiresistor:[10] a thin organic film contacted by two electrodes. In this case, the principle of sensing is the conductivity change due to chemical reactions or adsorption phenomena taking place in the film.

Materials Research Institute and School of Biological and Chemical Sciences, Queen Mary University of London, Mile End Road, London E1 4NS, United Kingdom.
E-mail: c.b.nielsen@qmul.ac.uk
† These authors contributed equally to this work.

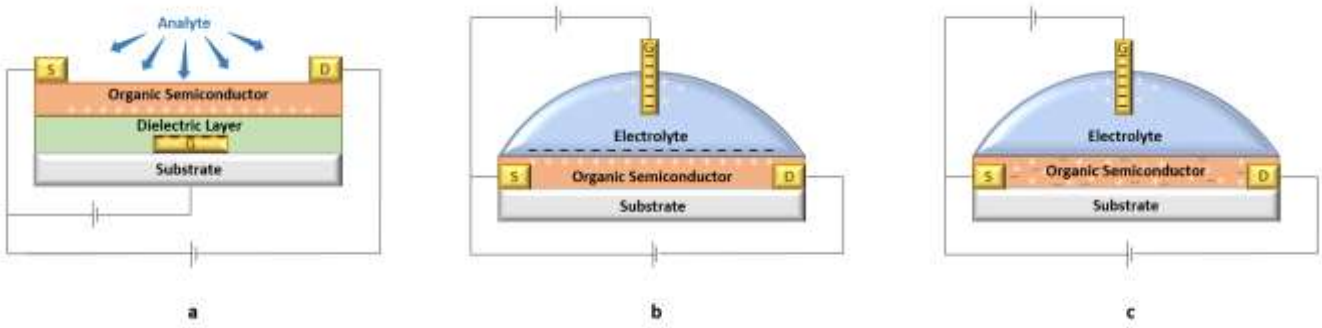

Figure 1. Operation of devices: (a) OFET; (b) EGOFET; (c) OECT; here exemplified for p-type transport in the channel.

One step further, in a three-terminal configuration (fig. 1a), a voltage can be applied between one pair of terminals ("source", S, and "drain", D), resulting in a current flowing through a conductive organic channel. Should a voltage be applied between another pair of terminals ("gate", G, and "source", S) in a perpendicular direction, charge carrier density increases or decreases in the layer of the organic channel that is closest to the dielectric. This way, current (output) can be modulated by the gate field effect (input), hence the name organic field effect transistor (OFET).[17] The sensitivity of the OFET sensor is given as the ratio of current change to gate bias change, i.e. the transconductance, g_m, $\partial I_D/\partial V_G$. Other important parameters are the threshold voltage (V_T) – the gate voltage that is required to initiate a conductive path – and the mobility (μ), the effectiveness with which charges can move through a material. Since the analyte can influence each of these factors differently, these devices contribute extra information over a simple resistor.[18]

Generally, the first OFET-sensors exposed the organic semiconducting layer to the analyte, in a bottom-gate configuration,[19] but alternative structures have been devised. For example, the gate electrode can be situated at the top of the device, separated from the semiconducting layer by an electrolyte (fig. 1b). Then, electrical double layers form at the gate-electrolyte and electrolyte-organic channel interfaces. These electrolyte-gated OFETs (EGOFETs) display much lower biasing voltages (<1 V) than traditional OFETs (>10 V) because of their higher capacitance. Another advantage derives from the possibility of functionalizing the gate electrode so that it interacts with the target analyte in the electrolyte.[20] Furthermore, if the ions of the electrolyte can penetrate the bulk of the organic channel, there can be charge compensation, actual redox reactions that change the carrier density of the semiconductor. This is the so-called organic electrochemical transistor (OECT, fig. 1c).[21]

Like EGOFETs, OECTs work under much lower voltages than OFETs.[22] In addition, the fact of separating gate and channel simplifies fabrication, for example, in arrays or integrated in a microfluidic channel. Both OFETs and OECTs feature enhanced sensitivity because, as transistors, they can work by amplifying a signal. However, while doping changes in OFETs are limited to an interfacial region, two dimensional in nature, OECTs can show much larger modulations, coming from doping over the bulk of the channel. Despite this, their response times are worse, but can be reduced down to milliseconds with a small distance gate-channel and short channel length.[23,24]

1.3 Strategies for the selective recognition of analytes or signals of biological interest

Electrical conductivity (σ, S m^{-1}) can be expressed as the relationship between elementary charge (e, 1.60 × 10^{-19} C), carrier concentration (n, m^{-3}) and mobility (μ, m^2 V^{-1} s^{-1}) (*Equation 1*). Elementary charge is a constant which denotes the electrical charge of a single proton or electron, while carrier concentration represents the quantity of charge carriers per unit of material.[25]

$$\sigma = ne\mu$$

Equation 1. Definition of electrical conductivity.

The advantage of organic electronic devices over other current technologies is that there is no need to tag the analyte with fluorophores, antibodies or radioisotopes; it is a label-free method. In these devices, the basis for a quantitative response to a biological analyte or event is the modulation of the current flowing through the channel, either due to changes in conductivity or effective gate voltage (fig. 2).[26–28] In terms of conductivity, mobility can be affected by alterations to morphology such as changes to grain boundaries or trapping charge carriers,[29] while carrier concentration can be affected by doping state. While the exact mechanism of the effect of biomarkers upon electrical conductivity is not always fully known,[27] semiconducting materials can still be applied successfully as sensors due to their observed effect.

The simplest approach is to use the organic semiconductor both as the electronic transducer and the sensing element. Generally, this leads to lack of selectivity, since most analytes affect carrier mobility by diffusing into the organic channel and also having a doping effect. In some cases, though, the affinity between the analyte and the organic semiconductor can be increased by the right choice of side chains, or the gate electrode itself can preferentially catalyse the oxidation of the analyte.[30–32] High selectivity and sensitivity have also been accessed by means of synthetic receptors; for example, a derivative of cucurbit[6]uril was layered on the organic channel for the recognition of acetylcholine.[33]

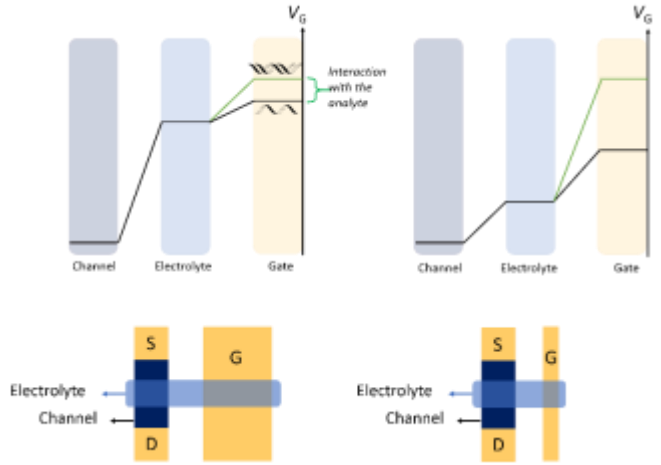

Figure 2. When the interaction with the analyte takes place at the gate, the sensitivity can be enhanced by reducing its area in comparison with the channel. Then, changes in the potential drop at the gate-electrolyte interface are maximised. Based on ref. 28.

However, for most requirements, biorecognition elements that specifically bind or transform the analyte such as enzymes, complementary nucleic acids strands or antibodies, are to be integrated. In order to preserve their conformation and function, these biomolecules are preferably immobilised, either at the gate or in the channel. Furthermore, in the case of redox enzymes, this step facilitates good electron relay with the electrode.[1] Organic materials can be electrochemically polymerised in the presence of the biomolecule so that it is entrapped in the matrix. Also, positively charged polymers in the matrix have been shown to improve electron transfer because of adsorption of the negatively charged enzyme.[34]

Alternatively, the biomolecule can be covalently bonded to functional groups on the surface.[18] One strategy is to generate a layer rich in carboxyl groups by plasma-enhanced chemical vapour deposition (PE-CVD) (fig. 3a). Then, the N-termini of the biomolecules can be chemically anchored via peptide coupling reactions.[35] In the case of proteins, direct coupling to free amino residues may lead to loss of activity. To overcome this issue, vesicles with phospholipids that carry different functionalities have been used as linkers. Some of the phospholipids are NH_2-appended and serve to anchor the vesicle to the COOH-rich surface of the organic channel (fig. 3b), while other phospholipids bear functional groups to attach the biorecognition elements.[36] The power of intercalating an insulating lipidic membrane between channel and gate is illustrated in recent work that uses a lipid monolayer at an aqueous-organic interface as a model to study bacterial membrane disruption by the action of antibiotics (fig. 3e).[37] In another approach, chemical anchoring is achieved by blending the organic semiconductor with poly(vinyl alcohol) (PVA); the alcohol groups provide access for silanization with an appropriate reagent that, in turn, possesses epoxide groups susceptible to opening by biomolecules (fig. 3c).[38] Finally, a different strategy exploits gold-sulphur chemistry; gold nanoparticles can be generated on the organic layer and linked to thiol-bearing biomolecules (fig. 3d).[39]

Increasing in complexity, organic devices have been proven to monitor the activity of whole cells, which can be applied to toxicology evaluation or drug discovery.[23,40,41] Every cell keeps a negative surface potential by actively pumping ions, and thus, changes in their ion fluxes reflect dysfunction. Generally, a monolayer of cells is grown between the channel and the gate, not only exerting an electrostatic field on the conducting material but also introducing a barrier for ion motion. In the case of electrogenic cells (myocytes and neurons), implantable devices have been used *in vivo*, performing better than traditional techniques to track neural and cardiac activity,[42–47] as will be discussed later.

The smart designs described so far can be further combined with microfluidics or textiles, allowing implementation for multianalyte sensing or wearable applications, such as a sweat monitoring band.[48]

1.4 Organic semiconductors

Electrical conduction in organic materials depends on conjugation, i.e. the overlap of molecular orbitals through systems of alternating simple and multiple bonds. The more extended the overlap, the narrower the energy difference between the lowest unoccupied and highest occupied molecular orbitals (LUMO and HOMO). Current will flow as long as there are empty states to which holes or electrons can move under an applied electric field. By nature, semiconductors cannot carry charge in their neutral state. While in theory, the application of thermal energy can excite electrons from the

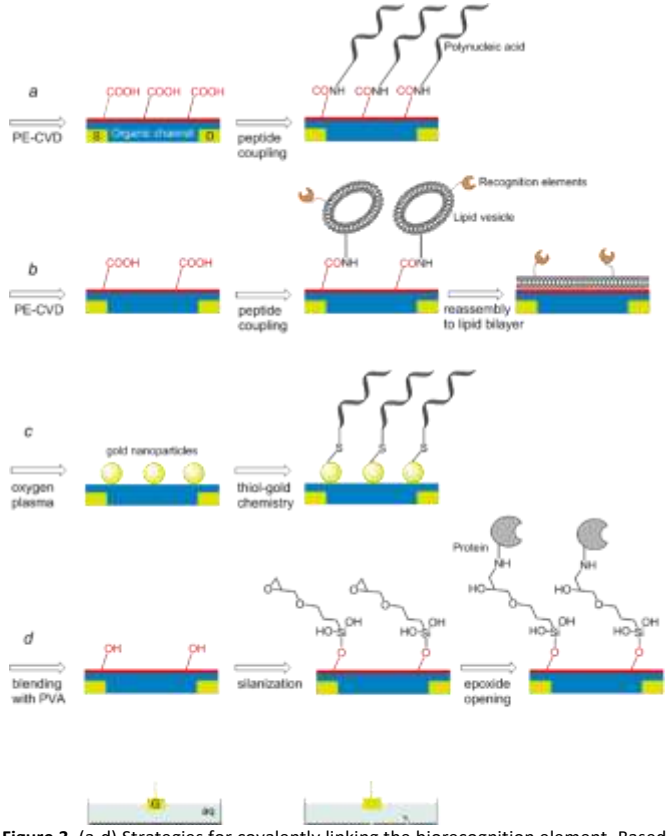

Figure 3. (a-d) Strategies for covalently linking the biorecognition element. Based on ref. 18. (e) Application of a lipid monolayer as a model to study bacterial membrane disruption.[37]

HOMO to the LUMO, in true semiconductors the bandgap is too large for this to be achieved (at room temperature, k_BT = 0.025 eV, while the bandgap is typically 0.7-3.0 eV). Therefore, these materials require ionization to enable charge transport, and this is achieved via doping with impurities which interact with the polymer to act as electron donors or acceptors. Materials can be categorised based on the type of charge carrier which they are able to transport. Those which can be oxidised to carry a positive charge (or "hole") are known as p-type, while those which are reduced to gain electrons are known as negative, n-type. In the case of organic materials, generally polycrystalline or amorphous, charge transport is a hopping process which leads to lower mobility values than those attained by band transport in inorganic crystalline solids. Hopping transport consists of sequential intermolecular redox transfers: electron transport occurs from anion radicals to neutral molecules through the LUMOs; hole transport occurs from neutral molecules to cation radicals through the HOMOs.

Several factors, all intertwined, allow the bandgap to be tuned at the synthetic stage, and simultaneously affect film morphology.[49,50] An effective approach has been to alternate electron-rich donor and electron-deficient acceptor units.[51,52] Another strategy intended to increase planarity is to hamper rotations between neighbouring units by connecting them with covalent bonds[53–55] or via non-covalent interactions.[56] Insertion of backbone substituents, such as side chains or fused aromatic rings, also plays a role in solubility and lamellar stacking orientation.[12] The building blocks derived have often been workhorses for parallel development of small molecules and polymers. The highest mobilities have been achieved with small molecules because of their higher crystallinity. This last fact can help when diffusion of species from the sample is to be prevented, usually a requirement in field-effect transistors. A high ON/OFF ratio of channel currents, typical of low-level doped small molecules, is another desired feature for these kinds of transistors. On the other hand, polymers with conducting behaviour or mixed ionic and electronic transport ability are ideal for OECTs interfacing with biological systems. On top of this, polymeric films are typically smoother, more reproducible and easier to process in various combinations with other materials. That is why the following examples for sensing applications abound more in polymers.

2. Polymers

The first realization of an intrinsically conductive polymer dates back to 1977, when polyacetylene $(CH)_x$ was partially oxidised (in other words, p-doped) with iodine, resulting in a dramatic increase of conductivity from ca. 10^{-5} S cm^{-1} to ca. 10^{3} S cm^{-1}, but it was not applicable at that time due to instability limitations.[57] From the 1980s onward, polymers based on heterocycles, such as polypyrrole (PPy), polyaniline (PAni) and polythiophenes, gave rise to a wide range of applications due to their higher stability and easier processing.

2.1 Polypyrrole (PPy)

The OECT was first conceived and developed in 1984 by White *et al.*.[21] The transistor comprised three gold microelectrodes coated in polypyrrole (chart 1a) as source, drain and gate. Oxidation of polypyrrole by input of the correct voltage at the gate resulted in amplification of the signal. While polypyrrole can be synthesised from pyrrole chemically, usually aided by an oxidising agent such as iron(III) chloride,[58,59] White *et al.* utilised electrochemical oxidation with 0.1 M tetrabutylammonium

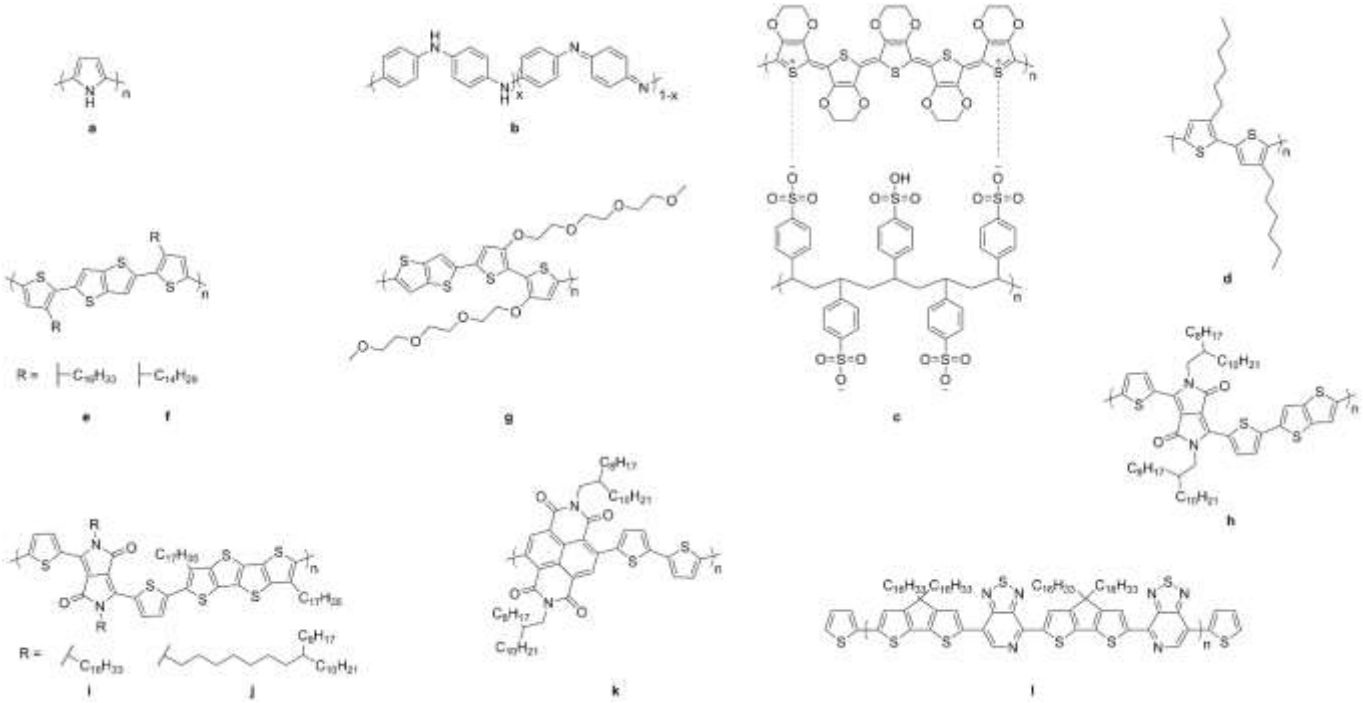

Chart 1. Conjugated polymers: (a) PPy; (b) PAni; (c) PEDOT:PSS; (d) P3HT; (e) PBTTT-C16; (f) PBTTT-C14; (g) p(g2T-TT); (h) DPP-DTT; (i,j) PTDPPTFT4; (k) P(NDI2OD-T2); (l) PCDTPT.

perchlorate in acetonitrile; electrochemical polymerization is preferable in the case of device fabrication due to the capacity to create high-quality, uniform films directly upon the electrode surface which is to be used in the device.[60] The advantages of polypyrrole as a semiconducting material include its relative simplicity, straightforward synthesis and thus minimal cost of production. However, White *et al.* reported that solutions must be sufficiently degassed to prevent irreversible oxidation, and have a lifetime use in the absence of oxygen of days. Thus, polypyrrole is perhaps less preferable for durable, easily processable device fabrication than some of its more air-stable alternatives.

Polypyrrole is also known to have poor solubility in many organic solvents,[61] and the absence of available functional groups for covalent modification limits the improvement of this, as well as the tuneability of the HOMO and LUMO (and so, bandgap) and the capacity for covalent functionalization with tailored groups to impart analyte targeting capability. Despite these issues, polypyrrole has been successfully applied in transistors for sensing application.

Polypyrrole has served as a versatile matrix to entrap relevant biomolecules, especially enzymes, during the electropolymerization step.[62,63] In fact, the first reports on glucose oxidase (GOx) immobilization for amperometric detection of glucose were based on polypyrrole,[64] and direct electron transfer between an enzyme and a conducting polymer was first demonstrated for a dehydrogenase entrapped in polypyrrole.[65,66] The benefit was to improve the performance of the sensor compared to the direct immobilization of the enzyme on the electrode surface, kindling the functionalization of polypyrrole with other biomolecules such as antibodies.[67,68]

As early as 1992, an OECT containing polypyrrole was developed for use as a penicillin sensor. By coating a polypyrrole-based OECT with a cross-linked penicillinase membrane, penicillin-G in contact with the device was converted to penicilloic acid via enzyme-catalysed hydrolysis. Due to the p-type nature of polypyrrole, the corresponding pH decrease increased the electron hole concentration, and thus, electrical conductivity, of the polypyrrole channel.[69]

Polypyrrole also shows very good biocompatibility, e.g. as a platform for growing and supporting the secretory function of cells,[70] or for stimulating and monitoring neural tissue.[71–73] A recent work[74] used a composite film of polypyrrole/polyol-borate embedded in an insulating elastomer to obtain a multielectrode array for conformal neural interfacing. The polymeric composite was the only conductor component in the array and made it possible to combine high electrical performance (the high charge injection capacity and low impedance resulting from the organic material increasing active area) and stretchability. The array was proven to record local field potentials on skeletal muscle.

However, while the properties of polypyrrole allow for its application in devices of this type, it is reported that the conductivity of polypyrrole is reduced in physiological conditions due to optimised performance at lower pH – and thus, it may not be suitable for use *in vivo*, which limits its potential for biological sensing.[22]

2.2 Polyaniline (PAni)

Following chart 1b, PAni oxidation states range from the fully reduced (x=1) to the fully oxidised form (x=0). The highest conductivity corresponds to an ideal intermediate oxidation state (x=0.5) called emeraldine.[57,75] Protonation of the base form depicted in the figure occurs preferentially at the imine N atoms of the oxidised units, thereby generating radical cations and an increase in conductivity of ten orders of magnitude. Therefore, doping of PAni is unique, in the sense that it is not only feasible by oxidation but also by an acid-base reaction. In line with this, PAni has been applied for pH sensing.[76–79] Early devices in the 1990s for the detection of other species, such as glucose, also relied on the local pH changes which originate from enzymatic reactions, though with poor limits of detection.[80] In a more sensitive approach, reduction of insulating oxidised PAni to its conducting form was coupled with the oxidation of glucose by mediation of GOx and tetrathiafulvalenium.[81]

Although a vast number of organic devices were initially based on PPy and PAni, films made solely of these polymers show fragility, poor stability and overoxidation, and low performance in physiological conditions, so the trend is to take advantage of their high conductivity by transforming them into hydrogels,[82,83] composites[84] and nanostructures.[30,75,85,86]

2.3 Poly(3,4-ethylenedioxythiophene) (PEDOT)

By far, the organic conductor with the widest range of applications is poly(3,4-ethylenedioxythiophene) (PEDOT), more specifically when its doped form is stabilised with the polyanion poly(styrene sulfonate)(PSS). The immobile, negatively charged PSS chains stabilise the positive charges that arise upon the oxidation of PEDOT and enable the transport of cations. The exact structure and charge carrier mechanisms of doped PEDOT:PSS are not fully known; while it is generally agreed that a quinoidal motif along the PEDOT backbone is formed upon interaction of sulfur groups on PEDOT with the charged sulfonate O^- of PSS, some propose that charge carrier capability arises from a bipolaron (chart 1c),[87] while others a polaron.[2,88]

Transistors based on conducting PEDOT:PSS work in depletion mode (fig. 4). Without a gate voltage, a hole current flows in the channel, whereas under a positive gate bias, cations from the electrolyte compensate the anions in the channel and the holes extracted at the drain are not resupplied at the source, suppressing the current. This ability of the electrolyte ions to modulate the film conductivity is the basis for translating an ionic signal into an electronic one.

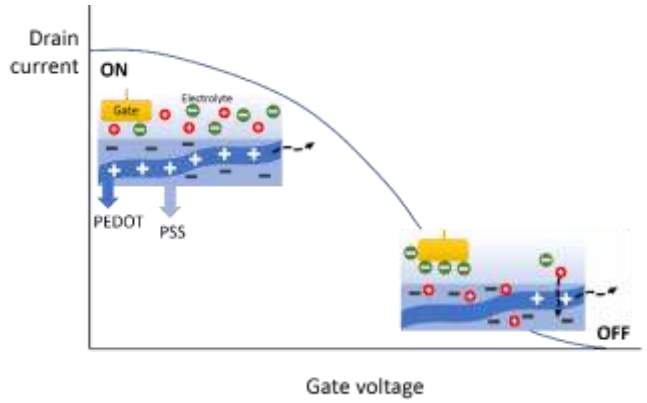

Figure 4. PEDOT:PSS is dedoped on applying a sufficiently positive voltage.

PEDOT:PSS is commercially available in the form of aqueous dispersions, which can be spin coated. The commercial synthesis consists of the polymerization of EDOT in the presence of PSS and sodium persulfate. Facile deposition of thin films can also be performed by electrochemical polymerization and vapour-phase polymerization.[8,89,90] Electropolymerization is easily carried out by exposing a solution with the monomer, the dopant and a supporting electrolyte to several oxidative cyclic voltammetry scans in a common electrochemical cell with three electrodes.

Most importantly, PEDOT:PSS displays outstanding intrinsic properties. Its hole conductivity can exceed 1000 S cm^{-1} [91] and the drift mobilities of small ions injected into hydrated PEDOT:PSS films are close to those in bulk water.[88,92] The dioxy bridge prevents the irreversible oxidation of the thiophene ring and provides good electrochemical stability in aqueous electrolytes, which is relevant for biological applications. All this combined with its biocompatibility,[93] has made PEDOT:PSS the choice for many biological sensing applications.[73–79]

For example, PEDOT:PSS electrodes have been used as surface electrodes for *in vivo* neural activity recording, where materials that guarantee good electrical contact are sought. Traditionally, multi-channel silicon probes ("Michigan probes") have been used for this purpose. However, the use of organic materials minimises the rejection response of the tissue, enables the combined detection of neurotransmitters and reduces the impedance at the interface with tissue. PEDOT:PSS is a good choice chiefly because of its highly doped state and good adaptation to the surface of the brain.

In a seminal work,[42] 4 µm-thick arrays of electrodes were spin coated and patterned on parylene substrates (individual electrodes with an area of 20 µm × 20 µm and a centre-to-centre distance of 60 µm, fig. 5a) and implanted *in vivo* onto the surface of the brain of rats, along with a silicon probe for comparison. Typical epileptic activity mimicked by the injection of bicuculline induced the same pattern of signals for both materials (fig. 5b), validating the use of PEDOT:PSS electrodes for electrocorticography.

This initial use as mere coating for electrodes was extended to OECT arrays as a means to locally amplify the biological signal. The action potentials of the neurons directly influence the

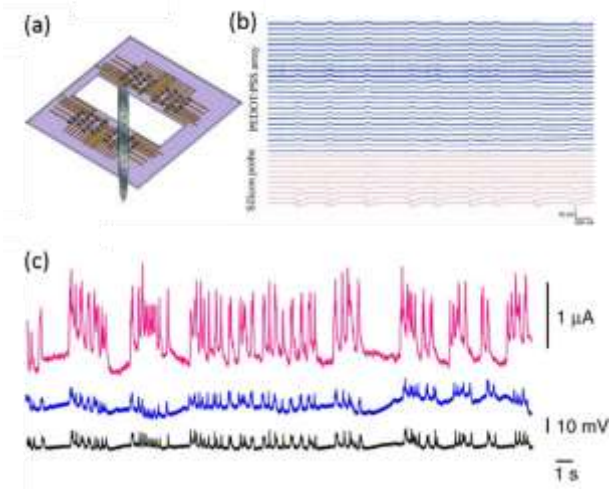

Figure 5. (a) Array of PEDOT:PSS surface electrodes with a silicon probe and (b) their recordings of induced epileptiform activity in rats, ordered according to the depth in the brain cortex. Reproduced with permission from ref. 42. Copyright 2011, John Wiley and Sons. (c) Recordings of epileptiform activity in "absence epilepsy" rats, from an OECT (pink), a PEDOT:PSS surface electrode (blue) and an Ir-penetrating electrode (black). Reproduced with permission from ref. 44. Copyright 2013, Springer Nature.

source-drain current in the transistor, enabling it to act as a potentiometric sensor.[94] Signal-to-noise ratios for the OECTs were 1.65-1.81 times better than for the surface electrodes, and higher than for the silicon probes[44] (fig. 5c). These arrays enabled neural recording for extended periods of time *in vivo*.[95]

Electric stimuli also occur in muscular tissue, where contraction is triggered by a depolarizing flux of cations into the cell, and consequently PEDOT:PSS OECTs have been applied for electrocardiographic recordings (ECG).[43] In this case, PEDOT:PSS was spin coated on a film of poly(L-lactide-co-glycolide) (PLGA), a synthetic bioresorbable polyester. By optimizing the film thickness (200 nm) and channel geometry, the transconductance and sensitivity were enhanced; signals as low as tens of microvolts were detected with a time response of milliseconds (fig. 6a, b). Then, a human ECG was recorded by directly attaching the transistor channel to the skin, which takes the role of the gate (fig. 6c). The measured current pattern and signal-to-noise ratio were comparable to the typical spikes of a

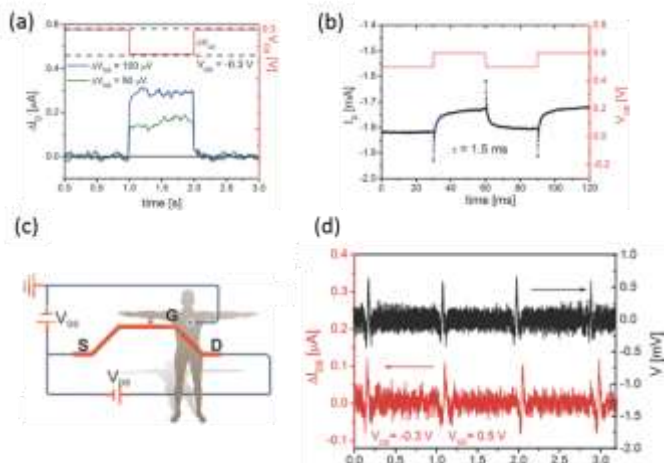

Figure 6. Application of a PEDOT:PSS OECT for ECG: (a) Potential changes as small as 50 µV result in measurable variations in drain current; (b) Gate voltage variations of 0.1 V are recorded with a fast response; (c) Diagram of the OECT connections for the human ECG; (d) Comparison between the OECT (red) and a standard potentiometric (black) recordings. Reproduced with permission from ref. 43. Copyright 2014, John Wiley and Sons.

potentiometric recording with Faradaic electrodes (fig. 6d). These reports showed a superior performance of PEDOT:PSS to amplify an ionic biological signal into an electronic signal, that relies on the ability of the film to uptake ions from the electrolyte in a volumetric capacitive process;[96] the thicker the film, the higher the transconductance and hence the sensitivity of the device.

Devices comprising PEDOT:PSS have also been developed to enable the selective detection of biomarkers including glucose,[26,27,97–101] ions,[102,103] DNA[104,105] and microRNA[106]. In many cases, incorporation of an interface is necessary in order to mediate interaction between the analyte and the semiconducting material.

For example, in the case of glucose, the majority of PEDOT-based sensing devices which have been developed in recent years incorporate the GOx enzyme, due to its high specificity for glucose and the associated functionality of oxidation allowing a straightforward conversion to electronic feedback. OECT devices have been fabricated which combine GOx with PEDOT[101] or PEDOT:PSS[26,27,97–100] all of which have been shown to exhibit a selective electrical response to the administration of glucose in aqueous solution.

However, criticism has emerged with regard to enzyme usage, citing matters such as instability,[107] gradual leaching over time, sensitivity to temperature, humidity, toxic chemicals, ionic detergents and pH,[108] delayed feedback response, and practical inconveniences such as complex immobilization procedures,[109] high cost, refreshment of single-use equipment and materials, and the necessity for the invasive obtainment of a fresh blood sample every time.[110] In 2017, an enzyme-based glucose sensor which averts many of these issues was developed via the introduction of a rhodium-carbon pellet-based system wherein a fresh sample of the enzyme is dispensed onto a passive three-electrode sensor prior to each measurement. This has even been extended to wireless transmission of data directly to a smartphone, for immediate feedback.[111] While this approach overcomes the problems associated with enzymatic degradation, gradual enzyme leaching, and hysteresis, it still requires the usage of a finger-prick blood test in addition to the necessity for continual maintenance of a supply of fresh enzyme pellets.[27] Thus, the search for a simpler and more robust, enzyme-free method of glucose detection continues. This is a developing field, but the first examples of enzyme-free glucose sensors based on PEDOT:PSS are now being reported.

In a notable example, in 2018 Sheng *et al.* fabricated an OECT which utilises $Ni(OH)_2$ and reduced graphene oxide (r-GO) alongside PEDOT to create a purely electrochemical sensor for glucose. A solution of EDOT and GO was ultrasonicated and electrodeposited onto a glassy carbon electrode, followed by electrodeposition of biocompatible $Ni(OH)_2$ nanoparticles. $Ni(OH)_2$ in combination with r-GO was shown to electro-catalytically oxidise glucose, negating the need for GOx incorporation. The device was able to detect glucose to a limit of 0.6 μM, in an ultrafast, selective and stable manner, and was successfully applied to detect glucose in human serum.[112]

The same year, Wustoni *et al.* created another enzyme-free glucose sensing OECT via a different approach: a one-pot polymerization of PEDOT:PSS alongside a phenylboronic acid-functionalised polyacrylamide gave a flexible electroactive gel, which was purported to have increased scalability compare to the previous example, due to the low abundance of nickel oxides in nature. Upon binding of glucose to the boronic acid moiety, the network swelled to facilitate diffusion of electrolyte ions into the gel and caused an increase in current. Thus, the device displayed a selective response for glucose, and this was demonstrated in a biologically-mimicking media containing the most abundant proteins from blood, haemoglobin and human serum albumin.[113]

In addition to glucose, PEDOT:PSS has been incorporated into multi-component OECT devices to sense other biomarkers. For instance, DNA and RNA are useful biomarkers in gene expression monitoring and microbial identification. In 2011, an OECT was applied to achieve a label-free DNA sensor with higher sensitivity than with OFETs,[114] following pioneering work by Krishnamoorthy *et al.*,[104] but by modifying the gate. The device was fabricated on polyethylene terephthalate (PET) and incorporated into a microfluidic channel, rendering it flexible, and a single-stranded DNA (ssDNA) segment was immobilised on the gold gate electrode. After a sequence of 6-hour hybridization with DNA targets and washing, transfer curves were recorded. Complementary DNA targets were shown to induce a larger shift to a higher gate voltage: 51 mV *vs* <5 mV for non-complementary DNA at the same concentration, 5 μM (fig. 7). A limit of detection of 1 nM was accomplished, but this was further decreased to 10 pM on augmenting the hybridization by electric field pulses. The sensing mechanism was explained in terms of the gate surface potential: negatively charged DNA molecules decrease the potential at the gold electrode, so the actual voltage for dedoping PEDOT must be shifted to higher values.

In a remarkable recent work,[115] both highly sensitive and specific detection of lactate was proven. Increased production of lactate *in vitro* was proposed as a biomarker for tumour malignancy. A key for this application was the design of a Wheatstone bridge circuit comprising two OECTs (fig. 8), to subtract the interferences arising from working with low volume cell culture samples, such as the oxidation of species on the electrode and the evaporation of the electrolyte. The PEDOT:PSS gate electrode of one of the OECTs was functionalised with a complex of lactate oxidase (LOx) and an electron transfer mediator (chitosan-ferrocene);[116] enzymatic oxidation of lactate relays electrons to the gate and results in dedoping of the PEDOT:PSS channel. On the other hand, a non-specific protein replaced LOx in the second “reference” OECT. This configuration enabled unambiguous identification of high lactate production from cancerous cells cultures relative to controls.

Lastly, the following separate contributions for detection of two neurotransmitters emphasise the versatility of PEDOT:PSS OECTs. The sensing principle for both adrenaline and dopamine was enzyme-free oxidation on the gate electrode. In the first case,[117] selectivity over other electro-oxidizable species, namely uric and ascorbic acids, was achieved by drop-coating the Pt gate with Nafion, which electrostatically attracts the

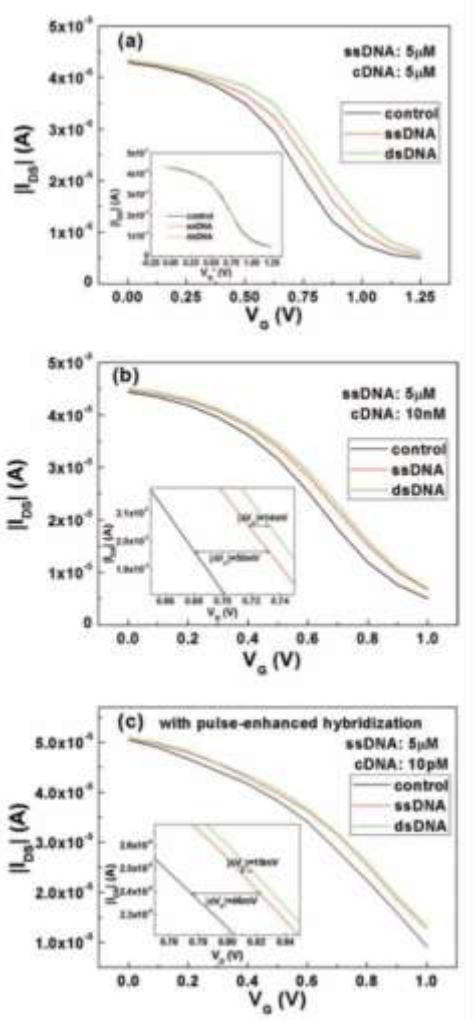

Figure 7. Transfer curves of a PEDOT:PSS OECT for label-free DNA detection resulting from hybridization times of 6 h at different target concentrations (a) (b) and from pulse-enhanced hybridization (c). Reproduced with permission from ref. 114. Copyright 2011, John Wiley and Sons.

protonated adrenaline at the pH of the phosphate buffer, while modifying the gate with single-walled carbon nanotubes improved sensitivity down to a detection limit of 0.1 nM, valid for current analytical requirements. As for the second contribution,[118] detection of dopamine in an all-PEDOT device was performed selectively without any functionalization of the electrodes. Instead, an instrumental recourse was applied. Transfer curves were recorded at a low-rate linear scan of potential for the mixture of dopamine and the interferents at the same time. Resolution was feasible since each analyte

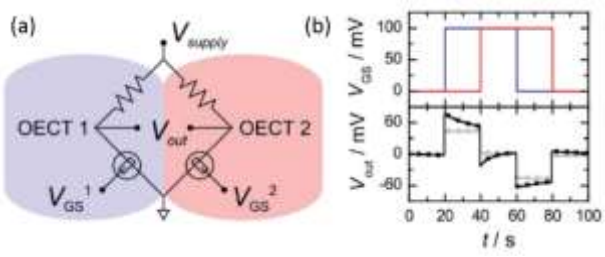

Figure 8. (a) The Wheatstone bridge sensor circuit devised for lactate detection; (b) Influence of potential pulses applied on the left (upper, blue) or right (upper, red) branches of the circuit on V_{out}. Reproduced with permission from ref. 115. Copyright 2016, John Wiley and Sons.

oxidation peak appears at different gate potentials for thermodynamic and kinetic reasons. This approach, though it neither meets biological analytical requirements (limit of detection was 6 μM) nor previous results with PEDOT OECT devices at the nanomolar level,[32] surpassed the sensitivity obtained with the more intricate technique differential pulse voltammetry.

In spite of its advantages, PEDOT:PSS has already been overtaken in terms of mobility by fused thiophene polymers,[12,119,120] and more versatile mechanical and functional behaviour is always desired. Another drawback of PEDOT:PSS is the acidity of PSS, which limits solution processability. These factors have prompted the development of new materials for organic electronic devices.

2.4 Poly(3-hexylthiophene) (P3HT)

Another high-profile p-type semiconducting material in popular use for transistor fabrication is poly(3-hexylthiophene) (P3HT, chart 1d). P3HT belongs to the family of 3-alkylthiophenes first synthesised by Elsenbaumer *et al.* in 1985, which, in addition to being some of the first environmentally stable and solution processable semiconducting polymers to be reported,[121] were regioregular in nature, a property caused by "head-to-tail" arrangement of alkyl chains of consecutive monomers as a result of their synthesis by nickel-catalysed Grignard metathesis (GRIM).[122] This property imbues the polymers with a relatively high charge-carrier mobility and thereby makes them excellent candidates for application in transistors. Thus, while there are several reported methods of polymerisation for the synthesis of P3HT,[123] perhaps the most enduring and worthy of note is its synthesis by GRIM metathesis, as first described by McCullough and Lowe in 1992.[124]

In the time since, P3HT has been incorporated into a range of transistor architectures for the purpose of sensing biologically relevant molecules. For example, in 2016, Han *et al.* created an OFET featuring a semiconducting channel of a P3HT:polystyrene blend, used as a gaseous ammonia sensor.[125] Ammonia can be considered of biological importance because there is evidence linking environmental ammonia with asthma and adverse respiratory symptoms,[126] in addition to arguments that exhaled ammonia as a metabolite may be used as a marker for monitoring these diseases.[127] Incorporation of polystyrene simultaneously increased the charge carrier mobility (from 0.01 $cm^2\ V^{-1}\ s^{-1}$ with pure P3HT to 0.03 $cm^2\ V^{-1}\ s^{-1}$ with a 1:4 blend of P3HT:polystyrene) and reduced the cost of the device in one efficient adaptation. Uniform films were deposited onto a poly(methyl methacrylate) (PMMA) dielectric layer via "on-the-fly" spin coating, in which the solution is deposited after high-speed rotation has already commenced, in order to create ultra-thin films.[128] No further biological interface was required and the gaseous ammonia was exposed directly to the film surface in controlled increasing concentrations from 0-50 ppm, resulting in a measurably decreased conductivity across the semiconducting channel. The authors attribute this to two factors: a reduction of hole concentration by the interaction of the lone pair of ammonia with P3HT, and trapped ammonia at

the boundary between the dielectric and semiconducting channel affecting the threshold voltage of the device.

In OFETs, charge accumulation occurs at the interface between the semiconducting layer and the dielectric, and thus diffusion of analytes into the semiconducting channel is required in order for an effect upon conductivity to be achieved.[18] In 2018, Wang *et al.* created an ammonia-sensing OFET which utilised an ultrathin (2.0 nm) P3HT semiconducting layer to facilitate analyte access to the interface, in order to avert this issue and improve sensitivity to the analyte. The ultrathin layers were obtained by vertical phase separation of polymer blends of P3HT and PMMA. Upon spin coating, these materials formed a bilayer with P3HT on the top, which were removed from the substrate in aqueous KOH, inverted onto a SiO_2/Si substrate, and etched with acetone to remove PMMA. The resulting OFET showed decreasing current when exposed to gaseous NH_3 for increasing periods of time, by the same mechanism described above.[129]

In addition to these examples of non-functionalised P3HT-based devices showing biological sensing capability, it is possible to impart specificity upon the device via incorporation of an interface using biological components, in order to target biomolecules of increased complexity. For example, a 2013 work by Casalini *et al.* presented a P3HT-based EGOFET which could selectively detect the neurotransmitter dopamine,[130] the imbalance of which is noted for its role in Parkinson's disease.[131] The device was the first OFET of any type constructed for this purpose, and was capable of responding to dopamine down to a picomolar concentration, thus exhibiting higher sensitivity than the PEDOT:PSS-based OECTs discussed in section 3.3. Furthermore, the use of a non-oxidative functionality averted the common problem of interference from other compounds of similar redox potential found in bodily fluids, such as ascorbic acid.[132] This was achieved via a self-assembled monolayer of cysteamine and 4-formylphenylboronic acid acting as an interface at the Au gate, which, upon covalent binding to dopamine, elicited the formation of a surface dipole which altered the conductivity across the P3HT channel.

The grafting of single-stranded DNA to the semiconducting surface can impart selectivity to analyte binding while also providing a mechanism through which the electrical signal of an OFET will be affected. Kergoat *et al.* demonstrated this in 2012; oligodeoxynucleotides (ODNs) were grafted to poly[3-(5-carboxypentyl)thiophene-2,5-diyl], an analogue of P3HT featuring a pendant carboxylic acid moiety, causing negative surface charges at the semiconducting layer and prohibiting current from flowing. Upon addition, in water or phosphate buffered saline (PBS), complementary HIV DNA strands hybridised with the ODNs to form rigid helical structures, the current decreased further. Specificity was demonstrated by the addition of random sequences, which were shown to have negligible effect.[133]

In 2018, Seshadri *et al.* designed an EGOFET capable of selective detection of the peptide procalcitonin (PCT),[134] which is an important biomarker in the diagnosis of sepsis.[135] In a fabrication process requiring only 45 min from start to finish, the spin coated P3HT layer was functionalised with a biorecognition interface comprising physically adsorbed PCT-specific antibodies and bovine serum albumin (BSA) to block the rest of the channel surface from interfering analytes. This ensured a decrease of measured current in the presence of PCT only, and with sensitivity down to the picomolar level in PBS mimicking the ionic strength and pH of human blood serum.

In nature, one of the strongest known non-covalent interactions is that of the vitamin biotin with the protein streptavidin (K_a = ca. 10^{15}).[136] This strong affinity makes them ideal candidates for a target-recognition molecule pairing in a biological sensing OFET, and as such they have been used to investigate and improve the functional characteristics of OFET devices. In 2017, Sportelli *et al.* found that layer-by-layer deposition of P3HT on top of streptavidin was a successful approach to obtaining selective biotin-sensing functionality to the picomolar level. P3HT was chosen for its porous morphology facilitating analyte diffusion through the channel to interact with the biomolecular layer.[137] Likewise, the same group built on this work the following year to determine that the addition of ZnO nanoparticles to the biological interface before semiconductor deposition increases the stability of the device from a few weeks to over a year.[138]

Unlike the capacitive processes in OFETs, the mode of operation of OECTs requires ions to diffuse evenly into the semiconducting layer in order for doping, and the subsequent change in conductivity, to occur.[20] A 2018 work by Pitsalidis *et al.* therefore selected P3HT as a suitable material for an OECT,[37] their reasoning citing its known ability to facilitate ion penetration by swelling in organic solvents.[139,140] Their P3HT-based OECT was able to measure modelled bacterial membrane disruption by application of antibiotics. The device featured a top-gate electrode exposed to an aqueous phase, with a dichloromethane phase below containing the electrolyte tetrabutylammonium hexafluorophosphate (TBA-PF_6) in contact with the semiconducting material. Application of a negative gate voltage caused ionic migration of TBA^+ into the aqueous phase and PF_6^- into the semiconducting material, the latter of which causes increased hole injection into P3HT from the source, and thus, and increased current is observed. When the DCM-H_2O interface was obstructed with a lipid monolayer mimicking a bacterial membrane, ionic migration is prohibited and observed current is decreased. Thus, upon addition of antimicrobial peptides polymyxin B or gramicidin A, the membrane was disrupted, allowing ion flow into the aqueous phase and semiconducting channel, successfully restoring the current. Devices such as this therefore provide a novel approach to the fast and accurate electrochemical determination of whether compounds may be useful as new antibiotics, a field of substantial urgency due to fast-emerging antibiotic resistance compounded by simultaneous slowing discovery of new drugs.[141]

Finally, the use of P3HT has extended beyond application in transistor-type devices. In 2018, Rezaei-Mazinani *et al.* fabricated an optical photodetector (OPD) comprising a P3HT blend with [6,6]-phenyl C60 butyric acid methyl ester (PCBM) as the photoactive layer, spin coated between an aluminium cathode and gold electrode. White light transmitted through

brain tissue was collected by a lens and optical changes were detected by the OPD, in order to monitor variations in cell volume associated with key processes such as hypoxia and metabolism.[142]

Herein, it is demonstrated that P3HT is a simple, reliable, and versatile material for applications across a wide range of device types for the sensing of different biological materials and processes.

2.5 Other thiophene-based polymers

While PEDOT:PSS and P3HT are perhaps the most well-known materials currently used in biological sensing devices, many other thiophene-based polymers have been applied for the same purpose to great effect, of which a selection are discussed below.

2.5.1. PBTTT-C16/C14

Crystallinity is in many cases key to charge carrier mobility. As such, larger crystalline domains in polymer films are associated with improved transistor performance. The fused thiophene moiety, thieno[3,2-b]thiophene, can be incorporated into polymers to achieve this characteristic. It features a linear backbone, low rotational variability, and often facilitates close π-stacking, all of which contribute to the formation of highly-ordered polymers. For example, in 2006, a series of p-type poly(2,5-bis(3-alkylthiophen-2-yl)thieno[3,2-*b*]thiophenes (PBTTT) were synthesised by McCulloch *et al.*, by a Stille cross-coupling between 2,5-bis(trimethylstannyl)thieno[3,2-*b*]thiophene and alkylated dibromobithiophenes. The authors observed that the polymers formed liquid crystals, resulting in large crystalline domains in the film after crystallization.[143]

These characteristics can be exploited in the fabrication of PBTTT-based sensing devices with enhanced properties in comparison to analogous devices featuring alternative semiconducting materials. In a 2014 study comparing the effectiveness of OFETs with semiconducting layers comprising either P3HT or poly(2,5-bis(3-hexadecylthiophen-2-yl)thieno[3,2-*b*]thiophene (PBTTT-C16, chart 1e), Manoli *et al.* found that PBTTT-C16-based devices displayed higher mobility than their P3HT counterparts (0.016 $cm^2\ V^{-1}\ s^{-1}$ and 0.00038 $cm^2\ V^{-1}\ s^{-1}$ respectively), and furthermore in the sensing of volatile organic compounds including ethanol, improved current amplification upon analyte exposure. This performance was attributed to the observation by scanning electron microscopy (SEM) of larger crystalline domains in PBTTT-C16 films than P3HT, as a result of its crystallization from the liquid-crystal phase.[144]

While good charge carrier mobility is vital to the functionality of transistor-type devices, application for sensing purposes also requires an optimized level of analyte exposure to the semiconducting channel; in other words, the surface area of the interface, or "roughness", should ideally be high, while maintaining crystallinity. In 2016, Yu *et al.* achieved this feat *via* the insertion of a hydrophobic buffer layer formed of octyltrichlorosilane (OTS), between the spin coated semiconducting layer poly(2,5-bis(3-tetradecylthiophen-2-yl)thieno[3,2-*b*]thiophene (PBTTT-C14, chart 1f) and the dielectric SiO_2 substrate. The effect was a decrease of the adhesion energy of PBTTT-C14/OTS to below the cohesive energy of the semiconducting layer (48.8 mN m^{-1} and 62.2 mN m^{-1} respectively), thereby increasing the roughness of the channel from 0.9 nm to 1.9 nm. Due to the insertion of the hydrophobic layer, this also improved the mobility from 0.007 $cm^2\ V^{-1}\ s^{-1}$ to 0.12 $cm^2\ V^{-1}\ s^{-1}$. A second buffer, the amorphous fluorinated polymer CYTOP, was also tested and while it gave well-developed, three-dimensional nanosized structures with a roughness of 6.1 nm, the corresponding disruption of overall crystallinity reduced the mobility to 0.013 $cm^2\ V^{-1}\ s^{-1}$ such that its usefulness as a sensing device was compromised. Thus, OTS provided the optimal balance between roughness and crystallinity, enabling the device to capture a large amount of ammonia gas, providing a highly sensitive response while incurring no meaningful detriment to mobility.[145] Indeed, when combined with a Pt electrode instead of the more common Au, PBTTT-C14 has been reported to have a charge carrier mobility up to 1 $cm^2\ V^{-1}\ s^{-1}$ on OTS-modified SiO_2.[146]

Research into the optimization of PBTTT-based devices continues today. In 2017, Sahu *et al.* created an ammonia sensor that was highly stable in ambient conditions, choosing CYTOP as the surface-modifying buffer, for its noted stability in addition to high gas capturing capability. Difficulties with earlier CYTOP/PBTTT morphology were circumvented via the use of the floating film transfer method (FTM) of deposition, to achieve an optimised thin-film thickness of 25 nm with high surface uniformity and terrace-phase morphology in the PBTTT film prior to stamping onto the device. The resulting sensor had a mobility of 0.050 $cm^2\ V^{-1}\ s^{-1}$ and showed negligible attrition of charge transfer characteristics when exposed to water vapour.[147] Furthermore, recent work by Boufflet *et al.* has demonstrated a fourfold improvement of charge carrier mobility (ca. 0.069 $cm^2\ V^{-1}\ s^{-1}$ to ca. 0.32 $cm^2\ V^{-1}\ s^{-1}$) upon modification of PBTTT-C16: introduction of a fluorine atom on the alkyl-thiophene units was linked to the formation of non-bonding S-F interactions, increasing the overall planarity of the polymer.[148]

2.5.2. p(g2T-TT)

While the thienothiophene moiety in PBTTT has low rotational variability due to its fused ring characteristic, the bithiophene moiety is still subject to twisting. This decreases backbone coplanarity and hence, reduces the overall mobility and effective conjugation length of the polymer. In order to avert this, Giovannitti *et al.* synthesised poly(2-(3,3'-bis(2-(2-(2-methoxyethoxy)ethoxy)ethoxy)-[2,2'-bithiophen]-5-yl)thieno[3,2-*b*]thiophene) (p(g2T-TT), chart 1g), which featured polar side chains based on ethylene glycol. The polymer was synthesised by a Stille coupling between 2,5-bis(trimethylstannyl)thieno[3,2-*b*]thiophene and glycolated dibromobithiophene. Intramolecular S-O interactions caused improved backbone coplanarity, and as a result a mobility of 0.95 $cm^2\ V^{-1}\ s^{-1}$ was achieved in an OECT without additives. The

authors also demonstrated that the additional oxygen atoms at intervals along the side chain were beneficial, because their interaction with an aqueous solvent and ionic dopants promotes ion penetration into the semiconducting channel.[14]
In 2018, the same group incorporated p(g2T-TT) into a device which was able to measure electroencephalography (EEG) signals at a low amplitude. Strategically positioned electrodes placed on a human scalp, including two behind the visual cortex, were connected to an OECT comprising spin coated p(g2T-TT). Local potential fluctuations resulting from the opening and closing of the eyes modulated the effective gate voltage, and thus the transistor was able to record neural activity while operating in the subthreshold region.[46] This low power, high voltage gain functionality is critical for implantable devices, and avoids the detrimental effects of high-power devices upon living tissue,[149] marking p(g2T-TT) as a good candidate for further use in low power biological sensing devices.

2.5.3. DPP-DTT

In 2010, Li *et al.* postulated that the inclusion of an electron-accepting comonomer into an otherwise p-type material would improve charge carrier transport by facilitating π-stacking and intermolecular interactions, in addition to increasing crystallinity. To that end, they utilised a Stille cross-coupling between bis(trimethylstannyl)thienothiophene and a brominated thiophene-diketopyrrolopyrrole (DPP) monomer, to create the solution processible, high molecular weight p-type polymer poly[[2,5-bis(2-octyldodecyl)-2,3,5,6- tetrahydro-3,6-dioxopyrrolo[3,4-*c*]pyrrole-1,4-diyl]-*alt*-[[2,2'-(2,5- thiophene)-bis-thieno(3,2-*b*)thiophene]-5,5'-diyl]] (DPP-DTT, chart 1h), which was highly crystalline, had a bandgap of 1.85 eV, and a hole mobility of 0.94 $cm^2 V^{-1} s^{-1}$ on OTS-modified SiO_2.[150]
The desirable properties of this polymer have led to its application in biological sensor devices such as an OFET reported in 2016 by Khim *et al*., who incorporated an ultrathin DPP-DTT layer of just 2.0 nm (controlled to 1-2 molecular layers) using a bar-coating deposition technique. The resulting device was shown by atomic force microscopy (AFM) and 2D grazing-incidence X-ray diffraction (GIXD) to be highly ordered in continuous "noodle-like" networks, a property difficult to achieve in ultrathin films created by other deposition techniques such as vacuum evaporation. To that end, the device showed sensitivity to gaseous ammonia up to 82 %, meaning that ammonia exposure decreased the channel current by 82 % in comparison to a "no ammonia" control. Furthermore, the OFET was shown to be responsive to ammonia where a device with a thick film semiconducting channel was not.[151] Another ammonia-sensing OFET featuring DPP-DTT and processed by bar-coating, by Ryu *et al.* the following year, improved this sensitivity to 87 %,[152] and both studies demonstrated a sensitivity for ammonia in the absence of such a response to other volatile gases such as ethanol and ethylene.
While many devices have been shown to possess the ability to sensitively detect biological molecules in an aqueous environment, the application of these devices alongside living tissue remains a problem, due to applied voltages above 0.3 V causing membrane rupturing and thus, cell death. Noting the polymer for its high crystallinity, in 2017, Zhang *et al.* used spin coated DPP-DTT as the semiconducting material for an OFET created to sense living cell detachment. The device in this work featured a solid-liquid OFET in which a dual-gate system was installed, enabling control of the channel threshold voltage by variation of a separate bottom-gate applied voltage from +3 to -3 V, while simultaneously maintaining operation at the top gate below the desired 0.3 V across the physiological sample. Living human mesenchymal stem cells (hMSCs) were cultivated upon the surface of a 25 nm DPP-DTT layer, effecting a decrease in the gate-field effect resulting from reduced ion concentration at the interface between the electrolyte and the semiconducting layer. Upon introduction of 50 µL trypsin to the electrolyte, at a bottom gate voltage of -3 V, the cells were detached from the substrate, and a corresponding restoration of current was observed. The dual-gated device displayed a threefold sensitivity and a faster response time than its single-gated analogue, and demonstrated high operational stability above a bottom-gate voltage of -3 V, which the authors attributed specifically to the use of DPP-DTT, citing its uniform, ordered morphology as observed by AFM and grazing incidence wide-angle X-ray scattering (GIWAXS).[153]
Since then, the biocompatibility of polymers of this type has been improved further. Citing the facile covalent functionalization of the DPP moiety as the reason for its suitability for this purpose, in 2018 Du *et al.* exchanged the C8/C10 side chain of a similar polymer, diketopyrrolopyrrole-terthiophene (DPP3T), for poly-$_L$-lysine. The effect was an increase in polymer hydrophilicity, which enabled improved ion permeation into the semiconducting channel, in addition to allowing live neuron attachment and growth upon the surface.[154] Thus DPP-DTT and its analogues remain strong contenders for future use either *in vivo* or in sensors involving live cell exposure.

2.5.4. PTDPPTFT4

Finally, extended systems of fused thiophenes are known to contribute to increased polymer rigidity and thus, improved π-stacking and charge carrier mobility properties. However, as fused ring count increases, solubility decreases. Thus, He *et al.* developed a family of alkyl-substituted fused thiophenes up to seven rings in length, which maintained solution processability while providing improved π-stacking and charge carrier transport.[155] The same group later showed that a 4-ring analogue featuring two C13 alkyl chains, FT4, when incorporated into semiconducting polymers improves transistor performance.[156]
The FT4 monomer, applied to the scaffold in section 2.5.3 above, gives the p-type semiconducting polymer poly(tetrathienoacene-diketopyrrolopyrrole) (PTDPPTFT4, chart 1i). First synthesised by Matthews *et al.* as recently as 2013, the polymer exhibits the "push-pull" system of DPP-DTT in addition to improved rigidity and stability provided by the FT4 moiety. Monomers of C16-alkylated bromothiophene-DPP and

C17-alkylated trimethylstannyl-FT4 were prepared in good yield, in a scalable, solution processable manner, followed by a Stille cross-coupling to afford the polymer. Although prone to aggregation, the polymer displayed fully reversible redox properties, high thermal stability up to 407 °C under N_2, a bandgap of 1.35 eV, and charge carrier mobility up to 2.1 $cm^2 V^{-1} s^{-1}$ on OTS-modified SiO_2, a marked improvement upon DPP-DTT.[157]

In a seminal work published in *Science* in 2018, Kim *et al.* utilised a C8/C10 branched analogue of PTDPPTFT4 (chart 1j) to form part of an artificial sensory nerve. Basing design on biological systems enables the production of simplified devices which can sense pressure and detect movement with small spatial resolution. PTDPPTFT4 was selected for its postsynaptic current decay time of ca. 2.35 ms, which is sufficiently comparable to that of biological afferent nerve synapses (1.5-5 ms). For comparison, the authors noted that the popular semiconductor P3HT had a decay time of ca. 299 s, far too long to be considered for a biologically-mimicking system. The three-component device comprised resistive pressure sensors, organic ring oscillators, and a synaptic transistor, the latter of these which contained PTDPPTFT4 as the semiconducting material alongside an ion-gel dielectric. The device was applied to distinguish braille lettering, detect object shape, and, by an electronic-biological hybrid reflex arc, cause stimulation of muscle movement when applied to a cockroach leg.[158] Furthermore, also in 2018, Pfattner *et al.* created a novel FET platform featuring spin coated PTDPPTFT4 alongside a polar fluorinated poly(vinylidene fluoride-co-hexafluoropropylene) dielectric, which gave a tunable photoresponse for operational bias voltages below 0.5 V. This property is of critical importance for application in biological sensors due to the small electrochemical window of aqueous media, and this work demonstrates the potential of PTDPPTFT4 as a promising candidate for application in biological sensing devices of the future.[159]

2.6 n-type polymers based on naphthalene diimides

Hitherto presented organic devices depend on hole transport (p-type). Although there is no physical basis that hole mobilities outperform electron mobilities, the development of n-type organic semiconductors has lagged, mainly because of ambient instability. For the material to be stable in an aqueous electrolyte and under air and moisture, the LUMO must lie lower than at least -4 eV.[160,161] Moreover, the material must be reversibly reduced and oxidised in the aqueous media.

Copolymerization of electron-deficient units, such as naphthalene and perylene diimides (NDIs and PDIs), isoindigo (IIG) or diketopyrrolopyrrole (DPP), with thiophene-based donor units have provided ambient stable organic n-type materials. A breakthrough was the discovery of poly([*N*,*N*′-bis(2-octyldodecyl)-naphthalene-1,4,5,8-bis(dicarboximide)-2,6-diyl]-*alt*-5,5′-(2,2′-bithiophene)), P(NDI2OD-T2) (chart 1k),[162] which has been recently modified in the first example of an n-type accumulation mode OECT for enzymatic sensing.[163] In this work, 90% of the original branched alkyl chains were substituted with polar glycol chains. Increasing glycol content enables electrochemical doping and operation as an OECT: the film swells more than 100% with a 100% glycol fraction; higher capacitance evidences more ion penetration; and reduction potential is lowered, yet electron mobility decreases too.[164] Furthermore, the glycol chains improve interaction with the enzyme, LOx, suppressing the need for a redox mediator or the chemical anchoring of the enzyme. The LOx catalysed oxidation of lactate directly relays electrons to the polymer backbone, cations are injected into the film and the device turns on. The device response is highly specific, reversible and sensitive, with a dynamic range from 10 µM to 10 mM.

The evolution of n-type materials has gone one step further with the application of the ladder-type polymer poly(benzimidazobenzophenantroline). Its higher planarity, rigidity and, hence, delocalization compared to the NDI-based polymers results in higher electron conductivity and stability. OECTs based on this polymer were combined with p-type OECTs to make complementary logic circuits,[165] thus enabling higher amplification with low power consumption and opening the door for more complex circuitries that can interface with biological systems.

3. Small molecules

Despite aggregation in solution often leading to reduced thin-film uniformity relative to polymeric materials,[166] small molecules have nonetheless provided a major contribution to the fabrication of organic semiconducting devices. The most comprehensive review to date identified 643 reported small molecules used in field-effect transistors, compared to only 66 distinct polymers for the same purpose.[167] In part this may be attributed to the relative ease of their synthesis, purification and characterization in comparison to polymers. Furthermore, to date the record hole mobility of a small molecule transistor is 43 $cm^2 V^{-1} s^{-1}$, in the form of a single-crystal rubrene (chart 2a) transistor by Yamagishi *et al*,[168] compared to 23.7 $cm^2 V^{-1} s^{-1}$, for a 50 kDa regioregular PCDTPT polymer (chart 1l) by Tseng *et al*.[169] Thus, it is important to consider small molecules in the examination of effective conjugated materials for organic bioelectronic devices.

3.1 Pentacene

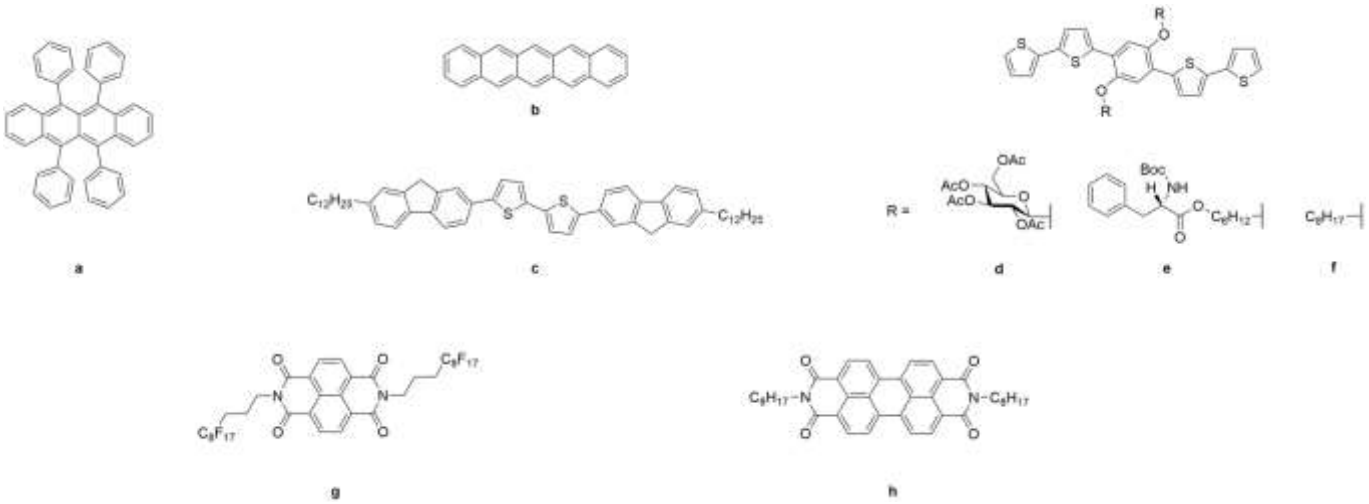

Chart 2. Conjugated small molecules: a) rubrene; b) pentacene; c) DDFTTF; d) PTG; e) PTA; f) PTO; g) 8-3 NTCDI; h) PTCDI-C8

The larger conjugation of pentacene (chart 2b) compared to smaller polycyclic aromatic hydrocarbons explains its superior optoelectronic properties, but also its lack of stability and solubility; acenes larger than six rings are elusive and barely investigated.[170] Shortly after pentacene transistors were first described in 1991,[171] high hole mobilities surpassing amorphous silicon (> 1 cm^2 V^{-1} s^{-1}) were being systematically attained,[172] prompting its use in fundamental studies as a prototype for organic semiconductors.[173,174] However, pentacene is very sensitive to degradation upon exposure to air and light, and bias stress limits its operating lifetime.[175,176] To ameliorate this, derivatives of pentacene have been synthesised,[177,178] yet most efforts have focused on modifying the device substrate to achieve low-voltage operation and passivation against ambient conditions.[179–181] Thus, it is reasonable that all the following applications of biological sensors consist of OFETs (no OECTs). A seminal work investigated label-free detection of DNA.[182] In this case, the sensing was based on the direct adsorption of DNA on the rough surface of pentacene due to hydrophobic interactions; the negatively-charged DNA molecules induce p-doping of the semiconductor and a large positive shift of the threshold voltage (fig. 9). Experimentally, DNA samples in buffer solution were pipetted on the organic film, air dried, rinsed and kept under nitrogen. The sensor response to DNA was measured in terms of the saturation current ratios. Interestingly, DNA hybridization was detected because the response to single stranded DNA was higher than that of double stranded, owing to a more efficient adsorption.

In a landmark contribution to antibody detection,[183] the pentacene channel was set between two perfluorinated polymer layers; one of them insulating (CYTOP), the other passivating (poly(perfluoro-1,3-dimethylcyclohexane), ppPFDMCH). The latter was functionalised with BSA for selective *in situ* detection of antiBSA in buffer solution. The fluoropolymer layers were very effective to preserve the electrical performance of pentacene: the CYTOP thin gate dielectric layer enabled the device to work at low voltages; and the passivating layer blocked degradation caused by water permeation.

In a final example, a pentacene EGOFET was applied as both the transducer and the stimulator of neural activity.[184] In this configuration, the direct exposure of an ultra-thin pentacene film to cell culture turned out to be advantageous. The capacitance in this interface is maximised in comparison with the use of a dielectric film, allowing functionality at low voltage (< 0.5 V) and a sensitive response to the small potential changes of the adhered cells. Pentacene mobility and morphology were stable in the cell culture conditions for up to nine days of device operation.

3.2 DDFTTF

One oligomer of interest which overcomes the stability issues of pentacene is 5,5'-bis-(7-dodecyl-9*H*-fluoren-2-yl)-2,2'-bithiophene (DDFTTF, chart 2c). The structure, comprising the electron-donating moieties fluorene and bithiophene, gives the molecule strong p-type character. First presented in 2006 by the Bao group,[185] the straightforward synthesis of DDFTTF via a Suzuki-Miyaura cross-coupling is based upon that of a previous series of analogues by the same group in 2003.[186] DDFTTF is notable for being highly water-stable, allowing its usage in devices with analytes in aqueous media, a crucial property of effective sensors applied to biological media. Thus, DDFTTF was

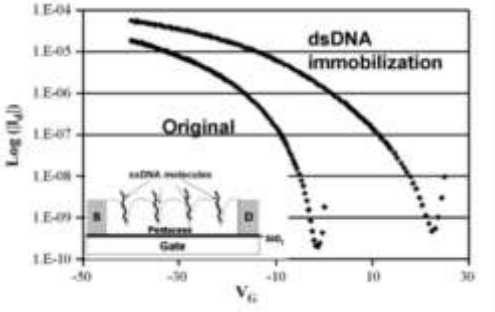

Figure 9. Transfer curves of a pentacene-based OFET for label-free DNA detection. Reproduced with permission from ref. 182. Copyright 2007 Elsevier.

the semiconducting material of choice in the fabrication of the first reported OFET which was functional and stable in aqueous

media.[187] Prior to this, analytes or dopants had only been exposed to OFETs after organic solution exposure[188] or as vapours.[189,190] Furthermore, the work demonstrated a capacity for biological sensing functionality in devices featuring DDFTTF; with the incorporation of an additional material as a biological interface being unnecessary, the DDFTTF OFET exhibited a sensitive, though non-selective, response to the biomolecules cysteine and glucose, as well as the chemical warfare agent trinitrobenzene, and the nerve agent metabolite analogue methylphosphonic acid. Explanations for this response were postulated to include interference of analytes as impurities with the electronic film (trinitrobenzene) and basic interaction of amine groups with H_3O^+ and positive charge carriers (cysteine).[187] DDFTTF has since been used in combination with synthetic peptide nucleic acid-functionalised poly(maleic anhydride), to create the first selective biological sensing OFET device which can detect specific target sequence DNA strands in situ. The device sensitivity was high enough to discriminate between strands of DNA with just one or two non-complementary bases to the targeting peptide nucleic acid, the first OFET to do so.[35] Unfortunately, DDFTTF is highly insoluble and thus not suited to large-scale production, because it must be processed by thermal evaporation.[191]

3.3 Phenylene thiophene oligomers

Sensing biological molecules with chiral selectivity has been achieved via covalent functionalization of side-chains with biological compounds of natural chirality. While covalent functionalization of polymers or oligomers is limited by steric hindrance in cases where large biological macromolecules such are proteins are the desired conjugate,[192] this technique has been applied successfully with smaller biomolecules such as glucose and amino acids. Torsi *et al.* constructed completely organic OFETs of p-type alkoxyphenylene-thiophene oligomers featuring covalently conjugated D-glucose (PTG, chart 2d) or L-phenylalanine (PTA, chart 2e), which were able to discriminate between the chiral natural products (R)-(−)- and (S)-(+)-carvone and (R)-(+)- and (S)-(−)-β-citronellol, respectively. Further to the problem of steric hindrance in synthesis mentioned above, Torsi *et al.* discovered that OFETs comprising functionalised PTA or PTG as the sole semiconducting material showed no field-effect amplified current, and thus could not be used as effective biological sensor devices. They concluded that this could also be attributed to steric hindrance and identified this as a general issue for any covalently-functionalised semiconducting material used in an OFET biological sensor. However, this problem was overcome via the novel structuring of the semiconducting channel as a bilayer featuring an alkoxy-substituted foundation (PTO, chart 2f) in contact with the dielectric layer, with the PTA or PTG layer staked on the PTO surface, in contact with the source and drain electrodes. Semiconducting materials were deposited using the Langmuir-Schaefer technique, and the resulting two-component channel successfully averted the issue of reduced conductivity. Oligomer synthesis was achieved using a Suzuki-Miyaura cross-coupling reaction, featuring a bithiophene pinacol boronic ester with a range of iodinated phenylene species featuring the noted functional groups. Overall this work demonstrated a straightforward, adaptable and novel method of producing a covalently functionalised, chiral-selective biological sensing device.[193]

3.4 n-type small molecules

There are a few examples of n-type small molecule devices for biochemical sensing based on naphthalene (chart 2g)[194] or perylene diimides (chart 2h).[195,196] Stable operation under ambient conditions has been achieved by intercalating a layer of the fluoropolymer CYTOP between the active layer and the dielectric in a bottom-gate, top contact configuration. This strategy was assayed for the detection of insulin dependent on its isoelectric point[195] and for the highly sensitive detection (20 pM) of glial fibrillary acidic protein as a biomarker of brain injury in combination with a p-type pentacene transistor.[194]

Conclusions and Outlook

The selection of electroactive materials for organic bioelectronics and more specifically for biological sensing as discussed herein has until recently been very limited. As a consequence, the majority of the early work in this field has been carried out with commercially available materials such as PEDOT:PSS and P3HT. Despite these early constraints, great progress has been made for instance by blending the electroactive materials with other functional components or by functionalising thin film surfaces with specific sensing moieties such as enzymes. In combination with the development of greatly improved electronic device geometries and architectures, many studies have underlined the potential of organic bioelectronics as a viable platform for selective sensing of numerous relevant biomarkers. More recently, the field has been enriched by organic semiconductors specifically tailored towards biological sensing applications. As a consequence, there are now both electron- and hole-transporting organic semiconductors that are fully compatible and operationally stable in aqueous milieu. This compatibility and drive towards mixed conduction of both ions and charges in the bulk material have in nearly all reports so far been achieved with glycolated polymer systems. Although it has afforded high-performing materials and opened up for new research directions, a number of aspects relating to the materials synthesis and characterisation still need to be studied and optimised further. From a synthesis point of view, the glycolated monomers are often difficult to purify adequately due to their ease of oxidation under ambient conditions and their lower crystallinity compared to alkylated counterparts. Moreover, the hygroscopic and chelating nature of the polar side chains pose an obstacle during the subsequent polymerisation where water and ion uptake can disrupt the stoichiometric balance while chelation of the Pd catalyst can likewise hinder a high degree of polymerisation. Where high degrees of polymerisation are nevertheless achieved, the resulting polymers often display poor solubility in common organic solvents due to their mixed hydrophobic-hydrophilic nature. As a consequence, solution-

based analytical techniques such as gel-permeation chromatography cannot be used reliably. By the same token, processability, in particular from more environmentally friendly non-chlorinated solvents, will be impaired by this lack of solubility for high molecular weight systems. More work is clearly needed to better understand and control these aspects. Efforts herein should also bring to light clearer structure-property relations and a better understanding of the role of polymer molecular weight on bioelectronic figures of merit.

Although the concept of mixed conduction of ions and charges is commonly addressed with molecular engineering, and in particular with glycolated side chains, it is worth pointing out that other approaches are also been explored. Faria and co-workers recently showed how several hydrophobic polymers, taken directly from the organic electronics community without laborious side-chain modifications, could display mixed conduction when interfaced with a non-aqueous liquid.[139] Work by Ginger and co-workers have likewise helped shed light on ion conduction in archetypical P3HT-based OECTs, which is highly dependent on the size of the ions and their hydration shells.[197] Such multi-faceted approaches and inter-disciplinary collaborations across (bio)chemistry, physics and engineering are crucial for rapid development of new materials, device architectures and sensing platforms.

We envision that this development of new bioelectronic materials will continue in the coming years with a further push for higher performing materials; this will for instance allow for greater sensitivities and further miniaturisation of devices in areas such as implantable sensors where device footprint is a crucial parameter. As the chemical methodologies become more robust and the design rules better understood, we also envision that a higher degree of structural complexity can be realised for example by incorporating specific sensing moieties directly onto the organic semiconductor.

As new high-performing materials pave their way into bioelectronic sensors, focus must also be placed on more thorough studies into the materials' ambient and operational stability, their biocompatibility and cytotoxicity and how these aspects can be optimised through molecular design and careful control of e.g. the material's purity. The monomeric constituents must be carefully chosen to ensure electrochemical stability and limit detrimental side reactions,[198] the materials' frontier energy levels must similarly be judiciously adjusted to prevent side reactions involving oxygen and water.[199,200] More biocompatible side-chains have also begun to receive attention,[154] but it is clear that much more work can be done in these areas to further elucidate structure-property relations and ultimately optimise the biosensing performance.

Conflicts of interest

There are no conflicts to declare.

Acknowledgements

The authors acknowledge the Academy of Medical Sciences & Wellcome Trust for financial support (SBF002/1158).

Notes and references

‡ Cells can grow on conducting polymer devices and these can be used to regulate their behaviour.[10] However, this review is focused on the converse direction, that is, when the bioreaction triggers a signal.

1 A. M. Pappa, O. Parlak, G. Scheiblin, P. Mailley, A. Salleo and R. M. Owens, *Trends Biotechnol.*, 2018, **36**, 45–59.

2 J. Rivnay, R. M. Owens and G. G. Malliaras, *Chem. Mater.*, 2014, **26**, 679–685.

3 C. Liao, M. Zhang, M. Y. Yao, T. Hua, L. Li and F. Yan, *Adv. Mater.*, 2015, **27**, 7493–7527.

4 T. Someya, Z. Bao and G. G. Malliaras, *Nature*, 2016, **540**, 379–385.

5 D. Venkateshvaran, M. Nikolka, A. Sadhanala, V. Lemaur, M. Zelazny, M. Kepa, M. Hurhangee, A. J. Kronemeijer, V. Pecunia, I. Nasrallah, I. Romanov, K. Broch, I. McCulloch, D. Emin, Y. Olivier, J. Cornil, D. Beljonne and H. Sirringhaus, *Nature*, 2014, **515**, 384–388.

6 M. Nikolka, I. Nasrallah, B. Rose, M. K. Ravva, K. Broch, A. Sadhanala, D. Harkin, J. Charmet, M. Hurhangee, A. Brown, S. Illig, P. Too, J. Jongman, I. McCulloch, J.-L. Bredas and H. Sirringhaus, *Nat. Mater.*, 2017, **16**, 356–362.

7 Y. Yuan, G. Giri, A. L. Ayzner, A. P. Zoombelt, S. C. B. Mannsfeld, J. Chen, D. Nordlund, M. F. Toney, J. Huang and Z. Bao, *Nat. Commun.*, 2014, **5**, 3005.

8 S. Inal, J. Rivnay, A.-O. Suiu, G. G. Malliaras and I. McCulloch, *Acc. Chem. Res.*, 2018, **51**, 1368–1376.

9 J. Xu, S. Wang, G. N. Wang, C. Zhu, S. Luo, L. Jin, X. Gu, S. Chen, V. R. Feig, J. W. F. To, S. Rondeau-Gagné, J. Park, B. C. Schroeder, C. Lu, J. Y. Oh, Y. Wang, Y. Kim, H. Yan, R. Sinclair, D. Zhou, G. Xue, B. Murmann, C. Linder, W. Cai, J. B.-H. Tok, J. W. Chung and Z. Bao, *Science*, 2017, **355**, 59–64.

10 D. T. Simon, E. O. Gabrielsson, K. Tybrandt and M. Berggren, *Chem. Rev.*, 2016, **116**, 13009–13041.

11 L. E. Freed, G. C. Engelmayr, J. T. Borenstein, F. T. Moutos and F. Guilak, *Adv. Mater.*, 2009, **21**, 3410–3418.

12 C. B. Nielsen, A. Giovannitti, D. T. Sbircea, E. Bandiello, M. R. Niazi, D. A. Hanifi, M. Sessolo, A. Amassian, G. G. Malliaras, J. Rivnay and I. McCulloch, *J. Am. Chem. Soc.*, 2016, **138**, 10252–10259.

13 A. Giovannitti, I. P. Maria, D. A. Hanifi, M. J. Donahue, D. Bryant, K. J. Barth, B. E. Makdah, A. Savva, D. Moia, M. Zetek, P. R. F. Barnes, O. G. Reid, S. Inal, G. Rumbles, G. G. Malliaras, J. Nelson, J. Rivnay and I. McCulloch, *Chem. Mater.*, 2018, **30**, 2945–2953.

14 A. Giovannitti, D.-T. Sbircea, S. Inal, C. B. Nielsen, E. Bandiello, D. A. Hanifi, M. Sessolo, G. G. Malliaras, I. McCulloch and J. Rivnay, *Proc. Natl. Acad. Sci.*, 2016, **113**, 12017–12022.

15 C. G. Tang, M. C. Y. Ang, K. K. Choo, V. Keerthi, J. K. Tan, M. N. Syafiqah, T. Kugler, J. H. Burroughes, R. Q. Png, L. L.

Chua and P. K. H. Ho, *Nature*, 2016, **539**, 536–540.
16 X. Cui, V. A. Lee, Y. Raphael, J. A. Wiler, J. F. Hetke, D. J. Anderson and D. C. Martin, *J. Biomed. Mater. Res.*, 2001, **56**, 261–272.
17 A. Tsumura, H. Koezuka and T. Ando, *Appl. Phys. Lett.*, 1986, **49**, 1210–1212.
18 L. Torsi, M. Magliulo, K. Manoli and G. Palazzo, *Chem. Soc. Rev.*, 2013, **42**, 8612–8628.
19 P. Lin and F. Yan, *Adv. Mater.*, 2012, **24**, 34–51.
20 D. Wang, V. Noël and B. Piro, *Electronics*, 2016, **5**, 9.
21 H. S. White, G. P. Kittlesen and M. S. Wrighton, *J. Am. Chem. Soc.*, 1984, **106**, 5375–5377.
22 X. Strakosas, M. Bongo and R. M. Owens, *J. Appl. Polym. Sci.*, 2015, **132**, 41735.
23 C. Yao, C. Xie, P. Lin, F. Yan, P. Huang and I.-M. Hsing, *Adv. Mater.*, 2013, **25**, 6575–6580.
24 D. Khodagholy, M. Gurfinkel, E. Stavrinidou, P. Leleux, T. Herve, S. Sanaur and G. G. Malliaras, *Appl. Phys. Lett.*, 2011, **99**, 163304.
25 C. Hilsum, *Electron. Lett.*, 1974, **10**, 259–260.
26 H. Tang, F. Yan, P. Lin, J. Xu and H. L. W. Chan, *Adv. Funct. Mater.*, 2011, **21**, 2264–2272.
27 D. A. Bernards, D. J. MacAya, M. Nikolou, J. A. Defranco, S. Takamatsu and G. G. Malliaras, *J. Mater. Chem.*, 2008, **18**, 116–120.
28 F. Cicoira, M. Sessolo, O. Yaghmazadeh, J. A. Defranco, S. Y. Yang and G. C. Malliaras, *Adv. Mater.*, 2010, **22**, 1012–1016.
29 L. Wang, D. Fine, S. I. Khondaker, T. Jung and A. Dodabalapur, *Sensors Actuators, B Chem.*, 2006, **113**, 539–544.
30 P. N. Bartlett, J. H. Wang and E. N. K. Wallace, *Chem. Commun.*, 1996, **0**, 359–360.
31 N. Coppedè, G. Tarabella, M. Villani, D. Calestani, S. Iannotta and A. Zappettini, *J. Mater. Chem. B*, 2014, **2**, 5620–5626.
32 H. Tang, P. Lin, H. L. W. Chan and F. Yan, *Biosens. Bioelectron.*, 2011, **26**, 4559–4563.
33 M. Jang, H. Kim, S. Lee, H. W. Kim, J. K. Khedkar, Y. M. Rhee, I. Hwang, K. Kim and J. H. Oh, *Adv. Funct. Mater.*, 2015, **25**, 4882–4888.
34 B. A. Kros, S. W. F. M. Van Hövell, N. A. J. M. Sommerdijk and R. J. M. Nolte, *Adv. Mater.*, 2001, **13**, 1555–1557.
35 H. Ullah Khan, M. E. Roberts, O. Johnson, R. Förch, W. Knoll and Z. Bao, *Adv. Mater.*, 2010, **22**, 4452–4456.
36 M. Magliulo, A. Mallardi, M. Y. Mulla, S. Cotrone, B. R. Pistillo, P. Favia, I. Vikholm-lundin, G. Palazzo and L. Torsi, *Adv. Mater.*, 2013, **25**, 2090–2094.
37 C. Pitsalidis, A.-M. Pappa, M. Porel, C. M. Artim, G. C. Faria, D. D. Duong, C. A. Alabi, S. Daniel, A. Salleo and R. M. Owens, *Adv. Mater.*, 2018, **30**, 1803130.
38 X. Strakosas, B. Wei, D. C. Martin and R. M. Owens, *J. Mater. Chem. B*, 2016, **4**, 4952–4968.
39 M. L. Hammock, O. Knopfmacher, B. D. Naab, J. B. H. Tok and Z. Bao, *ACS Nano*, 2013, **7**, 3970–3980.
40 P. Lin, F. Yan, J. Yu, H. L. W. Chan and M. Yang, *Adv. Mater.*, 2010, **22**, 3655–3660.
41 M. Ramuz, A. Hama, M. Huerta, J. Rivnay, P. Leleux and R. M. Owens, *Adv. Mater.*, 2014, **26**, 7083–7090.
42 D. Khodagholy, T. Doublet, M. Gurfinkel, P. Quilichini, E. Ismailova, P. Leleux, T. Herve, S. Sanaur, C. Bernard and G. G. Malliaras, *Adv. Mater.*, 2011, **23**, H268–H272.
43 A. Campana, T. Cramer, D. T. Simon, M. Berggren and F. Biscarini, *Adv. Mater.*, 2014, **26**, 3874–3878.
44 D. Khodagholy, T. Doublet, P. Quilichini, M. Gurfinkel, P. Leleux, A. Ghestem, E. Ismailova, T. Hervé, S. Sanaur, C. Bernard and G. G. Malliaras, *Nat. Commun.*, 2013, **4**, 1575.
45 P. Leleux, J. Rivnay, T. Lonjaret, J. M. Badier, C. Bénar, T. Hervé, P. Chauvel and G. G. Malliaras, *Adv. Healthc. Mater.*, 2015, **4**, 142–147.
46 V. Venkatraman, J. T. Friedlein, A. Giovannitti, I. P. Maria, I. McCulloch, R. R. McLeod and J. Rivnay, *Adv. Sci.*, 2018, **5**, 1800453.
47 C. Vallejo-Giraldo, A. Kelly and M. J. P. Biggs, *Drug Discov. Today*, 2014, **19**, 88–94.
48 W. Gao, S. Emaminejad, H. Y. Y. Nyein, S. Challa, K. Chen, A. Peck, H. M. Fahad, H. Ota, H. Shiraki, D. Kiriya, D. H. Lien, G. A. Brooks, R. W. Davis and A. Javey, *Nature*, 2016, **529**, 509–514.
49 Z. B. Henson, K. Müllen and G. C. Bazan, *Nat. Chem.*, 2012, **4**, 699–704.
50 Y.-J. Cheng, S.-H. Yang and C.-S. Hsu, *Chem. Rev.*, 2009, **109**, 5868–5923.
51 M. Wang, M. J. Ford, A. T. Lill, H. Phan, T. Q. Nguyen and G. C. Bazan, *Adv. Mater.*, 2017, **29**, 1603830.
52 L. Shi, Y. Guo, W. Hu and Y. Liu, *Mater. Chem. Front.*, 2017, **1**, 2423–2456.
53 Z. Cai, R. J. Vázquez, D. Zhao, L. Li, W. Y. Lo, N. Zhang, Q. Wu, B. Keller, A. Eshun, N. Abeyasinghe, H. Banaszak-Holl, T. Goodson and L. Yu, *Chem. Mater.*, 2017, **29**, 6726–6732.
54 J. Lee, A. J. Kalin, T. Yuan, M. Al-Hashimi and L. Fang, *Chem. Sci.*, 2017, **8**, 2503–2521.
55 Y. Wang, H. Guo, A. Harbuzaru, M. A. Uddin, I. Arrechea-Marcos, S. Ling, J. Yu, Y. Tang, H. Sun, J. T. López Navarrete, R. P. Ortiz, H. Y. Woo and X. Guo, *J. Am. Chem. Soc.*, 2018, **140**, 6095–6108.
56 H. Huang, L. Yang, A. Facchetti and T. J. Marks, *Chem. Rev.*, 2017, **117**, 10291–10318.
57 A. G. MacDiarmid, *Angew. Chemie - Int. Ed.*, 2001, **40**, 2581–2590.
58 S. P. Armes, *Synth. Met.*, 1987, **20**, 365–371.
59 J. Duchet, R. Legras and S. Demoustier-Champagne, *Synth. Met.*, 1998, **98**, 113–122.
60 G. Inzelt, M. Pineri, J. W. Schultze and M. A. Vorotyntsev, *Electrochim. Acta*, 2000, **45**, 2403–2421.
61 K. Li and B. Liu, *Chem. Soc. Rev.*, 2014, **43**, 6570–6597.
62 S. Sadki, P. Schottland, N. Brodie and G. Sabouraud, *Chem. Soc. Rev.*, 2000, **29**, 283–293.
63 S. Geetha, C. R. K. Rao, M. Vijayan and D. C. Trivedi, *Anal. Chim. Acta*, 2006, **568**, 119–125.
64 M. Umaña and J. Waller, *Anal. Chem.*, 1986, **58**, 2979–2983.
65 W. Schuhmann, H. Zimmermann, K. Habermüller and V. Laurinavicius, *Faraday Discuss.*, 2000, **116**, 245–255.

66 A. Ramanavicius, K. Habermuller, E. Csöregi, V. Laurinavicius and W. Schuhmann, *Anal. Chem.*, 1999, **71**, 3581–3586.

67 M. Gerard, A. Chaubey and B. D. Malhotra, *Biosens. Bioelectron.*, 2002, **17**, 345–359.

68 F. Wei, S. Cheng, Y. Korin, E. F. Reed, D. Gjertson, C. M. Ho, H. A. Gritsch and J. Veale, *Anal. Chem.*, 2012, **84**, 7933–7937.

69 M. Nishizawa, T. Matsue and I. Uchida, *Anal. Chem.*, 1992, **64**, 2642–2644.

70 T. Aoki, M. Tanino, K. Sanui, N. Ogata and K. Kumakura, *Biomaterials*, 1996, **17**, 1971–1974.

71 X. Wang, X. Gu, C. Yuan, S. Chen, P. Zhang, T. Zhang, J. Yao, F. Chen and G. Chen, *J. Biomed. Mater. Res. - Part A*, 2004, **68A**, 411–422.

72 P. M. George, A. W. Lyckman, D. A. LaVan, A. Hegde, Y. Leung, R. Avasare, C. Testa, P. M. Alexander, R. Langer and M. Sur, *Biomaterials*, 2005, **26**, 3511–3519.

73 T. Nyberg, O. Inganäs and H. Jerregård, *Biomed. Microdevices*, 2002, **4**, 43–52.

74 L. Guo, M. Ma, N. Zhang, R. Langer and D. G. Anderson, *Adv. Mater.*, 2014, **26**, 1427–1433.

75 E. Song and J.-W. Choi, *Nanomaterials*, 2013, **3**, 498–523.

76 P. Mostafalu, A. Tamayol, R. Rahimi, M. Ochoa, A. Khalilpour, G. Kiaee, I. K. Yazdi, S. Bagherifard, M. R. Dokmeci, B. Ziaie, S. R. Sonkusale and A. Khademhosseini, *Small*, 2018, **14**, 1703509.

77 M. Kaempgen and S. Roth, *J. Electroanal. Chem.*, 2006, **586**, 72–76.

78 E. W. Paul, A. J. Ricco and M. S. Wrighton, *J. Phys. Chem.*, 1985, **89**, 1441–1447.

79 R. Rahimi, M. Ochoa, T. Parupudi, X. Zhao, I. K. Yazdi, M. R. Dokmeci, A. Tamayol, A. Khademhosseini and B. Ziaie, *Sensors Actuators, B Chem.*, 2016, **229**, 609–617.

80 H. Sangodkar, S. Sukeerthi, R. S. Srinivasa, R. Lal and A. Q. Contractor, *Anal. Chem.*, 1996, **68**, 779–783.

81 P. N. Bartlett, J. H. Wang and W. James, *Analyst*, 1998, **123**, 387–392.

82 L. Pan, G. Yu, D. Zhai, H. R. Lee, W. Zhao, N. Liu, H. Wang, B. C.-K. Tee, Y. Shi, Y. Cui and Z. Bao, *Proc. Natl. Acad. Sci.*, 2012, **109**, 9287–9292.

83 N. Mano, E. Y. Joung, J. Tarver, Y. L. Loo and A. Heller, *J. Am. Chem. Soc.*, 2007, **129**, 7006–7007.

84 J. Wang and N. Hui, *Bioelectrochemistry*, 2019, **125**, 90–96.

85 D. Li, J. Huang and R. B. Kaner, *Acc. Chem. Res.*, 2009, **42**, 135–145.

86 J. Huang, S. Virji, B. H. Weiller and R. B. Kaner, *J. Am. Chem. Soc.*, 2003, **125**, 314–315.

87 R. Gangopadhyay, B. Das and M. R. Molla, *RSC Adv.*, 2014, **4**, 43912–43920.

88 J. Rivnay, S. Inal, B. A. Collins, M. Sessolo, E. Stavrinidou, X. Strakosas, C. Tassone, D. M. Delongchamp and G. G. Malliaras, *Nat. Commun.*, 2016, **7**, 11287.

89 L. B. Groenendaal, F. Jonas, D. Freitag, H. Pielartzik and J. R. Reynolds, *Adv. Mater.*, 2000, **12**, 481–494.

90 B. Winther-Jensen and K. West, *Macromolecules*, 2004, **37**, 4538–4543.

91 Y. Wang, C. Zhu, R. Pfattner, H. Yan, L. Jin, S. Chen, F. Molina-Lopez, F. Lissel, J. Liu, N. I. Rabiah, Z. Chen, J. W. Chung, C. Linder, M. F. Toney, B. Murmann and Z. Bao, *Sci. Adv.*, 2017, **3**, e1602076.

92 E. Stavrinidou, P. Leleux, H. Rajaona, D. Khodagholy, J. Rivnay, M. Lindau, S. Sanaur and G. G. Malliaras, *Adv. Mater.*, 2013, **25**, 4488–4493.

93 M. Berggren and A. Richter-Dahlfors, *Adv. Mater.*, 2007, **19**, 3201–3213.

94 P. Fromherz, A. Offenhäusser, T. Vetter and J. Weis, *Science*, 1991, **252**, 1290–1293.

95 D. Khodagholy, J. N. Gelinas, T. Thesen, W. Doyle, O. Devinsky, G. G. Malliaras and G. Buzsáki, *Nat. Neurosci.*, 2015, **18**, 310–315.

96 J. Rivnay, P. Leleux, M. Ferro, M. Sessolo, A. Williamson, D. A. Koutsouras, D. Khodagholy, M. Ramuz, X. Strakosas, R. M. Owens, C. Benar, J. M. Badier, C. Bernard and G. G. Malliaras, *Sci. Adv.*, 2015, **1**, e1400251.

97 N. Y. Shim, D. A. Bernards, D. J. Macaya, J. A. DeFranco, M. Nikolou, R. M. Owens and G. G. Malliaras, *Sensors*, 2009, **9**, 9896–9902.

98 C. Liao, M. Zhang, L. Niu, Z. Zheng and F. Yan, *J. Mater. Chem. B*, 2013, **1**, 3820–3829.

99 J. Liu, M. Agarwal and K. Varahramyan, *Sensors Actuators, B Chem.*, 2008, **135**, 195–199.

100 S. Y. Yang, F. Cicoira, R. Byrne, F. Benito-Lopez, D. Diamond, R. M. Owens and G. G. Malliaras, *Chem. Commun.*, 2010, **46**, 7972–7974.

101 Y. Kim, J. Do, J. Kim, S. Y. Yang, G. G. Malliaras, C. K. Ober and E. Kim, *Jpn. J. Appl. Phys.*, 2010, **49**, 01AE10.

102 Z. Mousavi, A. Ekholm, J. Bobacka and A. Ivaska, *Electroanalysis*, 2009, **21**, 472–479.

103 M. Sessolo, J. Rivnay, E. Bandiello, G. G. Malliaras and H. J. Bolink, *Adv. Mater.*, 2014, **26**, 4803–4807.

104 K. Krishnamoorthy, R. S. Gokhale, A. Q. Contractor and A. Kumar, *Chem. Commun.*, 2004, **0**, 820–821.

105 J. Song, P. Lin, Y.-F. Ruan, W.-W. Zhao, W. Wei, J. Hu, S. Ke, X. Zeng, J.-J. Xu, H.-Y. Chen, W. Ren and F. Yan, *Adv. Healthc. Mater.*, 2018, **7**, 1800536.

106 J. Peng, T. He, Y. Sun, Y. Liu, Q. Cao, Q. Wang and H. Tang, *Microchim. Acta*, 2018, **185**, 408.

107 A. Heller and B. Feldman, *Chem. Rev.*, 2008, **108**, 2482–2505.

108 H.-C. Wang, H. Zhou, B. Chen, P. M. Mendes, J. S. Fossey, T. D. James and Y.-T. Long, *Analyst*, 2013, **138**, 7146–7151.

109 M. Yang, Y. Yang, Y. Liu, G. Shen and R. Yu, *Biosens. Bioelectron.*, 2006, **21**, 1125–1131.

110 A. Salek-Maghsoudi, F. Vakhshiteh, R. Torabi, S. Hassani, M. R. Ganjali, P. Norouzi, M. Hosseini and M. Abdollahi, *Biosens. Bioelectron.*, 2018, **99**, 122–135.

111 A. J. Bandodkar, S. Imani, R. Nuñez-Flores, R. Kumar, C. Wang, A. M. V. Mohan, J. Wang and P. P. Mercier, *Biosens. Bioelectron.*, 2018, **101**, 181–187.

112 L. Sheng, Z. Li, A. Meng and Q. Xu, *Sensors Actuators, B Chem.*, 2018, **254**, 1206–1215.

113 S. Wustoni, A. Savva, R. Sun, E. Bihar and S. Inal, *Adv. Mater. Interfaces*, 2018, 1800928.

114 P. Lin, X. Luo, I.-M. Hsing and F. Yan, *Adv. Mater.*, 2011, **23**, 4035–4040.

115 M. Braendlein, A.-M. Pappa, M. Ferro, A. Lopresti, C. Acquaviva, E. Mamessier, G. G. Malliaras and R. M. Owens, *Adv. Mater.*, 2017, **29**, 1605744.

116 A.-M. Pappa, V. F. Curto, M. Braendlein, X. Strakosas, M. J. Donahue, M. Fiocchi, G. G. Malliaras and R. M. Owens, *Adv. Healthc. Mater.*, 2016, **5**, 2295–2302.

117 C. H. Mak, C. Liao, Y. Fu, M. Zhang, C. Y. Tang, Y. H. Tsang, H. L. W. Chan and F. Yan, *J. Mater. Chem. C*, 2015, **3**, 6532–6538.

118 I. Gualandi, D. Tonelli, F. Mariani, E. Scavetta, M. Marzocchi and B. Fraboni, *Sci. Rep.*, 2016, **6**, 35419.

119 Y. Olivier, D. Niedzialek, V. Lemaur, W. Pisula, K. Müllen, U. Koldemir, J. R. Reynolds, R. Lazzaroni, J. Cornil and D. Beljonne, *Adv. Mater.*, 2014, **26**, 2119–2136.

120 S. Inal, G. G. Malliaras and J. Rivnay, *Nat. Commun.*, 2017, **8**, 1767.

121 R. L. Elsenbaumer, K. Y. Jen and R. Oboodi, *Synth. Met.*, 1986, **15**, 169–174.

122 M. C. Stefan, M. P. Bhatt, P. Sista and H. D. Magurudeniya, *Polym. Chem.*, 2012, **3**, 1693–1701.

123 A. Marrocchi, D. Lanari, A. Facchetti and L. Vaccaro, *Energy Environ. Sci.*, 2012, **5**, 8457–8474.

124 R. D. McCullough and R. D. Lowe, *J. Chem. Soc., Chem. Commun.*, 1992, **0**, 70–72.

125 S. Han, X. Zhuang, W. Shi, X. Yang, L. Li and J. Yu, *Sensors Actuators, B Chem.*, 2016, **225**, 10–15.

126 S. G. Ballal, B. A. Ali, A. A. Albar, H. O. Ahmed and A. Y. Al-Hasan, *Int. J. Tuberc. Lung Dis.*, 1998, **2**, 330–335.

127 S. A. Kharitonov and P. J. Barnes, *Biomarkers*, 2002, **7**, 1–32.

128 F. J. Zhang, C. Di, N. Berdunov, Y. Hu, Y. Hu, X. Gao, Q. Meng, H. Sirringhaus and D. Zhu, *Adv. Mater.*, 2013, **25**, 1401–1407.

129 X. Wang, Z. Liu, S. Wei, F. Ge, L. Liu, G. Zhang, Y. Ding and L. Qiu, *Synth. Met.*, 2018, **244**, 20–26.

130 S. Casalini, F. Leonardi, T. Cramer and F. Biscarini, *Org. Electron.*, 2013, **14**, 156–163.

131 J. D. Elsworth and R. H. Roth, *Exp. Neurol.*, 1997, **144**, 4–9.

132 F. Malem and D. Mandler, *Anal. Chem.*, 1993, **65**, 37–41.

133 L. Kergoat, B. Piro, M. Berggren, M.-C. Pham, A. Yassar and G. Horowitz, *Org. Electron.*, 2012, **13**, 1–6.

134 P. Seshadri, K. Manoli, N. Schneiderhan-Marra, U. Anthes, P. Wierzchowiec, K. Bonrad, C. Di Franco and L. Torsi, *Biosens. Bioelectron.*, 2018, **104**, 113–119.

135 R. Sager, A. Kutz, B. Mueller and P. Schuetz, *BMC Med.*, 2017, **15**, 15.

136 M. González, L. A. Bagatolli, I. Echabe, J. L. R. Arrondo, C. E. Argaraña, C. R. Cantor and G. D. Fidelio, *J. Biol. Chem.*, 1997, **272**, 11288–11294.

137 M. C. Sportelli, R. A. Picca, K. Manoli, M. Re, E. Pesce, L. Tapfer, C. Di Franco, N. Cioffi and L. Torsi, *Appl. Surf. Sci.*, 2017, **420**, 313–322.

138 R. A. Picca, K. Manoli, A. Luciano, M. C. Sportelli, G. Palazzo, L. Torsi and N. Cioffi, *Sensors Actuators, B Chem.*, 2018, **274**, 210–217.

139 D. T. Duong, Y. Tuchman, P. Chakthranont, P. Cavassin, R. Colucci, T. F. Jaramillo, A. Salleo and G. C. Faria, *Adv. Electron. Mater.*, 2018, **4**, 1800090.

140 D. Ofer, R. M. Crooks and M. S. Wrighton, *J. Am. Chem. Soc.*, 1990, **112**, 7869–7879.

141 J. Davies and D. Davies, *Microbiol. Mol. Biol. Rev.*, 2010, **74**, 417–433.

142 S. Rezaei-Mazinani, A. I. Ivanov, C. M. Proctor, P. Gkoupidenis, C. Bernard, G. G. Malliaras and E. Ismailova, *Adv. Mater. Technol.*, 2018, **3**, 1700333.

143 I. McCulloch, M. Heeney, C. Bailey, K. Genevicius, I. MacDonald, M. Shkunov, D. Sparrowe, S. Tierney, R. Wagner, W. Zhang, M. L. Chabinyc, R. J. Kline, M. D. McGehee and M. F. Toney, *Nat. Mater.*, 2006, **5**, 328–333.

144 K. Manoli, L. M. Dumitru, M. Y. Mulla, M. Magliulo, C. Di Franco, M. V. Santacroce, G. Scamarcio and L. Torsi, *Sensors*, 2014, **14**, 16869–16880.

145 S. H. Yu, J. Cho, K. M. Sim, J. U. Ha and D. S. Chung, *ACS Appl. Mater. Interfaces*, 2016, **8**, 6570–6576.

146 B. H. Hamadani, D. J. Gundlach, I. McCulloch and M. Heeney, *Appl. Phys. Lett.*, 2007, **91**, 243512.

147 P. K. Sahu, M. Pandey, C. Kumar, S. S. Pandey, W. Takashima, V. N. Mishra and R. Prakash, *Sensors Actuators, B Chem.*, 2017, **246**, 243–251.

148 P. Boufflet, Y. Han, Z. Fei, N. D. Treat, R. Li, D.-M. Smilgies, N. Stingelin, T. D. Anthopoulos and M. Heeney, *Adv. Funct. Mater.*, 2015, **25**, 7038–7048.

149 T. M. Seese, H. Harasaki, G. M. Saidel and C. R. Davies, *Lab. Investig.*, 1998, **78**, 1553–1562.

150 Y. Li, S. P. Singh and P. Sonar, *Adv. Mater.*, 2010, **22**, 4862–4866.

151 D. Khim, G. S. Ryu, W.-T. Park, H. Kim, M. Lee and Y.-Y. Noh, *Adv. Mater.*, 2016, **28**, 2752–2759.

152 G.-S. Ryu, B. Nketia-Yawson, E.-Y. Choi and Y.-Y. Noh, *Org. Electron.*, 2017, **51**, 264–268.

153 Y. Zhang, J. Li, R. Li, D. T. Sbircea, A. Giovannitti, J. Xu, H. Xu, G. Zhou, L. Bian, I. McCulloch and N. Zhao, *ACS Appl. Mater. Interfaces*, 2017, **9**, 38687–38694.

154 W. Du, D. Ohayon, C. Combe, L. Mottier, I. P. Maria, R. S. Ashraf, H. Fiumelli, S. Inal and I. McCulloch, *Chem. Mater.*, 2018, **30**, 6164–6172.

155 M. He and F. Zhang, *J. Org. Chem.*, 2007, **72**, 442–451.

156 H. F. Hon, V. A. Pozdin, A. Amassian, G. G. Malliaras, D.-M. Smilgies, M. He, S. Gasper, F. Zhang and M. Sorensen, *J. Am. Chem. Soc.*, 2008, **130**, 13202–13203.

157 J. R. Matthews, W. Niu, A. Tandia, A. L. Wallace, J. Hu, W.-Y. Lee, G. Giri, S. C. B. Mannsfeld, Y. Xie, S. Cai, H. H. Fong, Z. Bao and M. He, *Chem. Mater.*, 2013, **25**, 782–789.

158 Y. Kim, A. Chortos, W. Xu, Y. Liu, J. Y. Oh, D. Son, J. Kang, A. M. Foudeh, C. Zhu, Y. Lee, S. Niu, J. Liu, R. Pfattner, Z. Bao and T.-W. Lee, *Science*, 2018, **360**, 998–1003.

159 R. Pfattner, A. M. Foudeh, C. Liong, L. Bettinson, A. C. Hinckley, D. Kong and Z. Bao, *Adv. Electron. Mater.*, 2018, **4**, 1700326.

160 H. Sun, J. Gerasimov, M. Berggren and S. Fabiano, *J. Mater. Chem. C*, 2018, **6**, 11778–11784.

161 J. Dhar, U. Salzner and S. Patil, *J. Mater. Chem. C*, 2017, **5**,

7404–7430.
162 H. Yan, Z. Chen, Y. Zheng, C. Newman, J. R. Quinn, F. Dötz, M. Kastler and A. Facchetti, *Nature*, 2009, **457**, 679–686.
163 A.-M. Pappa, D. Ohayon, A. Giovannitti, I. P. Maria, A. Savva, I. Uguz, J. Rivnay, I. Mcculloch, R. M. Owens and S. Inal, *Sci. Adv.*, 2018, **4**, eaat0911.
164 A. Giovannitti, C. B. Nielsen, D. T. Sbircea, S. Inal, M. Donahue, M. R. Niazi, D. A. Hanifi, A. Amassian, G. G. Malliaras, J. Rivnay and I. McCulloch, *Nat. Commun.*, 2016, **7**, 13066.
165 H. Sun, M. Vagin, S. Wang, X. Crispin, R. Forchheimer, M. Berggren and S. Fabiano, *Adv. Mater.*, 2018, **30**, 1704916.
166 W. Xiao, J. Wang, H. Li, L. Liang, X. Xiang, X. Chen, J. Li, Z. Lu and W. Li, *RSC Adv.*, 2018, **8**, 23546–23554.
167 C. Wang, H. Dong, W. Hu, Y. Liu and D. Zhu, *Chem. Rev.*, 2012, **112**, 2208–2267.
168 M. Yamagishi, J. Takeya, Y. Tominari, Y. Nakazawa, T. Kuroda, S. Ikehata, M. Uno, T. Nishikawa and T. Kawase, *Appl. Phys. Lett.*, 2007, **90**, 182117.
169 H. R. Tseng, H. Phan, C. Luo, M. Wang, L. A. Perez, S. N. Patel, L. Ying, E. J. Kramer, T. Q. Nguyen, G. C. Bazan and A. J. Heeger, *Adv. Mater.*, 2014, **26**, 2993–2998.
170 J. E. Anthony, *Angew. Chemie - Int. Ed.*, 2008, **47**, 452–483.
171 G. Horowitz, D. Fichou, X. Peng and F. Garnier, *Synth. Met.*, 1991, **41**, 1127–1130.
172 T. W. Kelley, P. F. Baude, C. Gerlach, D. E. Ender, D. Muyres, M. A. Haase, D. E. Vogel and S. D. Theiss, *Chem. Mater.*, 2004, **16**, 4413–4422.
173 A. A. Virkar, S. Mannsfeld, Z. Bao and N. Stingelin, *Adv. Mater.*, 2010, **22**, 3857–3875.
174 D. Braga and G. Horowitz, *Adv. Mater.*, 2009, **21**, 1473–1486.
175 M. E. Roberts, S. C. B. Mannsfeld, M. L. Tang and Z. Bao, *Chem. Mater.*, 2008, **20**, 7332–7338.
176 Y. Qiu, Y. Hu, G. Dong, L. Wang, J. Xie and Y. Ma, *Appl. Phys. Lett.*, 2003, **83**, 1644–1646.
177 W. Fudickar and T. Linker, *J. Am. Chem. Soc.*, 2012, **134**, 15071–15082.
178 J. E. Anthony, J. S. Brooks, D. L. Eaton and S. R. Parkin, *J. Am. Chem. Soc.*, 2001, **123**, 9482–9483.
179 R. Lassnig, M. Hollerer, B. Striedinger, A. Fian, B. Stadlober and A. Winkler, *Org. Electron. physics, Mater. Appl.*, 2015, **26**, 420–428.
180 Y. W. Wang, G.-Y. Tseng, L.-Y. Chiu, B.-R. Lin, Y.-Y. Lin, T.-W. Haung, W.-Y. Chou, L. Horng and H.-L. Cheng, *J. Mater. Chem. C*, 2014, **2**, 7752–7760.
181 H. U. Khan, M. E. Roberts, W. Knoll and Z. Bao, *Chem. Mater.*, 2011, **23**, 1946–1953.
182 Q. Zhang and V. Subramanian, *Biosens. Bioelectron.*, 2007, **22**, 3182–3187.
183 H. U. Khan, J. Jang, J.-J. Kim and W. Knoll, *J. Am. Chem. Soc.*, 2011, **133**, 2170–2176.
184 T. Cramer, B. Chelli, M. Murgia, M. Barbalinardo, E. Bystrenova, D. M. de Leeuw and F. Biscarini, *Phys. Chem. Chem. Phys.*, 2013, **15**, 3897–3905.
185 D. M. DeLongchamp, M. M. Ling, Y. Jung, D. A. Fischer, M. E. Roberts, E. K. Lin and Z. Bao, *J. Am. Chem. Soc.*, 2006, **128**, 16579–16586.
186 H. Meng, J. Zheng, A. J. Lovinger, B.-C. Wang, P. G. Van Patten and Z. Bao, *Chem. Mater.*, 2003, **15**, 1778–1787.
187 M. E. Roberts, S. C. B. Mannsfeld, N. Queraltó, C. Reese, J. Locklin, W. Knoll and Z. Bao, *Proc. Natl. Acad. Sci. U. S. A.*, 2008, **105**, 12134–12139.
188 X. Guo, M. Myers, S. Xiao, M. Lefenfeld, R. Steiner, G. S. Tulevski, J. Tang, J. Baumert, F. Leibfarth, J. T. Yardley, M. L. Steigerwald, P. Kim and C. Nuckolls, *Proc. Natl. Acad. Sci.*, 2006, **103**, 11452–11456.
189 B. Crone, A. Dodabalapur, A. Gelperin, L. Torsi, H. E. Katz, A. J. Lovinger and Z. Bao, *Appl. Phys. Lett.*, 2001, **78**, 2229–2231.
190 L. Torsi, A. Dodabalapur, L. Sabbatini and P. G. Zambonin, *Sensors Actuators, B Chem.*, 2000, **67**, 312–316.
191 O. Knopfmacher, M. L. Hammock, A. L. Appleton, G. Schwartz, J. Mei, T. Lei, J. Pei and Z. Bao, *Nat. Commun.*, 2014, **5**, 2954.
192 I. Cobo, M. Li, B. S. Sumerlin and S. Perrier, *Nat. Mater.*, 2015, **14**, 143–149.
193 L. Torsi, G. M. Farinola, F. Marinelli, M. C. Tanese, O. H. Omar, L. Valli, F. Babudri, F. Palmisano, P. G. Zambonin and F. Naso, *Nat. Mater.*, 2008, **7**, 412–417.
194 W. Huang, K. Besar, R. LeCover, P. Dulloor, J. Sinha, J. F. Martínez Hardigree, C. Pick, J. Swavola, A. D. Everett, J. Frechette, M. Bevan and H. E. Katz, *Chem. Sci.*, 2014, **5**, 416–426.
195 M. Ramesh, H. C. Lin and C.-W. Chu, *J. Mater. Chem.*, 2012, **22**, 16506–16513.
196 V. Benfenati, S. Toffanin, S. Bonetti, G. Turatti, A. Pistone, M. Chiappalone, A. Sagnella, A. Stefani, G. Generali, G. Ruani, D. Saguatti, R. Zamboni and M. Muccini, *Nat. Mater.*, 2013, **12**, 672–680.
197 L. Q. Flagg, R. Giridharagopal, J. Guo and D. S. Ginger, *Chem. Mater.*, 2018, **30**, 5380–5389.
198 A. Giovannitti, K. J. Thorley, C. B. Nielsen, J. Li, M. J. Donahue, G. G. Malliaras, J. Rivnay and I. McCulloch, *Adv. Funct. Mater.*, 2018, **28**, 1706325.
199 D. M. de Leeuw, M. M. J. Simenon, A.R. Brown, R. E. F. Einerhand, *Synthetic Metals*, 1997, **87**, 53–59.
200 B. Winther-Jensen, O. Winther-Jensen, M. Forsyth and D. R. MacFarlane, *Science*, 2008, **321**, 671–674.